

Supporting Information

Iron-Catalyzed 1,2-Selective Hydroboration of *N*-Heteroarenes

Fanjun Zhang,[‡] Heng Song,[‡] Xuewen Zhuang, Chen-Ho Tung and Wenguang Wang*

School of Chemistry and Chemical Engineering, Shandong University, 27 South Shanda Road, Jinan, 250100, China. Email: wwg@sdu.edu.cn

Table of contents

1. General information	S2
2. Experimental procedures	S3
2.1 Synthesis of [Cp*(Ph ₂ PC ₆ H ₄ S)Fe] ₂ (μ-N ₂).....	S3
2.2 Screening of reaction conditions	S5
2.3 General procedures for the hydroboration of <i>N</i> -heteroarenes	S6
3. Characterization data of <i>N</i> -boryl-dihydropyridines	S10
4. Reactions of <i>N</i> -heteroarenes with HBpin without 1	S17
5. Reaction of [Cp*(Ph ₂ PC ₆ H ₄ S)Fe] ₂ (μ-N ₂) with isoquinoline and pyridines.....	S18
6. X-ray crystal structure determinations	S20
7. Iron-catalyzed hydroboration of 2-methylpyridine with HBpin	S21
8. Stoichiometric reaction of [Cp*(Ph ₂ PC ₆ H ₄ S)Fe(C ₉ H ₇ N)] (6) with HBpin	S22
8.1 Reaction of [Cp*(Ph ₂ PC ₆ H ₄ S)Fe(C ₉ H ₇ N)] with HBpin.....	S22
8.2 Reaction of [Cp*(Ph ₂ PC ₆ H ₄ S)Fe(C ₉ H ₇ N)] with HBpin and CO	S23
8.3 Reaction of [Cp*(Ph ₂ PC ₆ H ₄ S)Fe(C ₉ H ₇ N)] with 9-BBN	S24
9. Kinetic experiments	S26
9.1 Pre-catalyst 1 rate order assessment based on initial-rate kinetics.....	S27
9.2 Isoquinoline rate order assessment	S28
9.3 HBpin rate order assessment	S29
9.4 Determination of the kinetic isotope effect	S30
10. ¹ H NMR and ¹³ C spectra.....	S31
11. X-ray crystal structure analysis.....	S62
12. Reference	S69

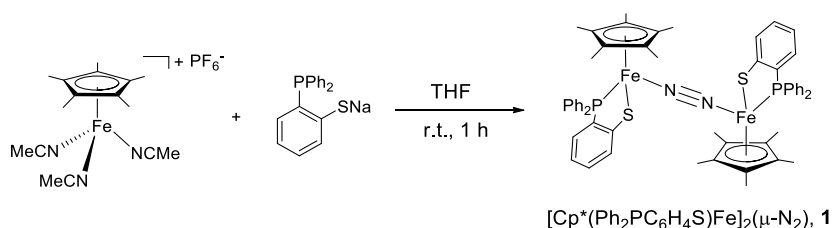
1. General information

All reactions were performed in flame-dried glassware using standard Schlenk techniques or in a glovebox under nitrogen atmosphere. Toluene, hexane and acetonitrile were dried and degassed by Solvent Purification Systems (Innovative Technology). C₆D₆ was dried with 4Å molecular sieves and degassed by freeze-pump-thaw methods. Tetraethylsilane, borane reagents as well as pyridines, quinolines, isoquinolines, phenanthridine and methyl-1*H*-benzo[d]imidazole were purchased from commercial suppliers. Borane reagents stored at -30 °C under N₂ atmosphere in glovebox and used as received. All solid heteroarenes were dried under vacuum and liquid heteroarenes were distilled prior to use. The 2-(diphenylphosphino)benzenethiol (Ph₂PC₆H₄SH)¹ and [Cp*Fe(NCMe)₃]PF₆² were prepared according to reported procedures. NMR spectra were recorded in J. Young tube on Bruker 500 (500 MHz for ¹H, 126 MHz for ¹³C, 160 MHz for ¹¹B) spectrometers. Chemical shifts for ¹H and ¹³C spectra were referenced to residual solvent resonances and are reported relative to tetramethylsilane. BF₃·OEt₂ was used as external standard for ¹¹B NMR.

2. Experimental procedures

2.1 Synthesis of $[\text{Cp}^*(\text{Ph}_2\text{PC}_6\text{H}_4\text{S})\text{Fe}]_2(\mu\text{-N}_2)$

$\text{Ph}_2\text{PC}_6\text{H}_4\text{SNa}$. NaH (0.09 g, 3.74 mmol) was added to a THF solution of $\text{Ph}_2\text{PC}_6\text{H}_4\text{SH}$ (1.0 g, 3.40 mmol) under nitrogen. The mixture was stirred at room temperature for 1 h and filtered through a short pad of celite. The filtrate was concentrated in vacuo and the product was recrystallized in THF/hexane to give $\text{Ph}_2\text{PC}_6\text{H}_4\text{SNa}$ as white solid (1.02 g, 95%). ^1H NMR (500 MHz, acetone- d_6): δ 7.37 (m, 1H), 7.24 (m, 10H), 6.75 (m, 1H), 6.45 (m, 1H), 6.32 (m, 1H). ^{31}P NMR: δ -15.4.



$[\text{Cp}^*(\text{Ph}_2\text{PC}_6\text{H}_4\text{S})\text{Fe}]_2(\mu\text{-N}_2)$, **1.** $\text{Ph}_2\text{PC}_6\text{H}_4\text{SNa}$ (252 mg, 0.83 mmol) in 5 mL THF was added to the solution of $[\text{Cp}^*\text{Fe}(\text{NCMe})_3]\text{PF}_6$ (380 mg, 0.83 mmol) in 30 mL THF, the color turned to red brown immediately. After stirring for 1 h at room temperature, the volatile was removed under vacuum, and the residue was extracted with toluene (10 mL). The resulting toluene solution was concentrated, layered with pentane and cooled at $-30\text{ }^\circ\text{C}$ to give $[\text{Cp}^*(\text{Ph}_2\text{PC}_6\text{H}_4\text{S})\text{Fe}]_2(\mu\text{-N}_2)$ (310 mg, yield 75%) as brown solid. Anal. Calcd for $\text{C}_{56}\text{H}_{58}\text{Fe}_2\text{N}_2\text{P}_2\text{S}_2$: C, 67.48; H, 5.87; N, 2.81. Found: C, 67.65; H, 5.62; N, 2.91. Raman ($\nu_{\text{N}=\text{N}}$, cm^{-1}): 2016. ESI-MS calcd. for $[\text{Cp}^*(\text{Ph}_2\text{PC}_6\text{H}_4\text{S})\text{Fe}]$, 484.1077; found, 484.1063. Magnetic susceptibility (μ_{eff} , C_6D_6 , $23\text{ }^\circ\text{C}$): $2.79\text{ }\mu_{\text{B}}$.

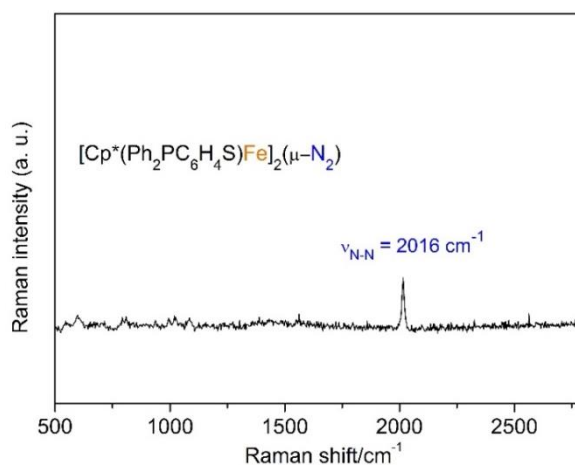


Figure S1. Raman spectrum of $[\text{Cp}^*(\text{Ph}_2\text{PC}_6\text{H}_4\text{S})\text{Fe}]_2(\mu\text{-N}_2)$ taken with 785 nm laser excitation.

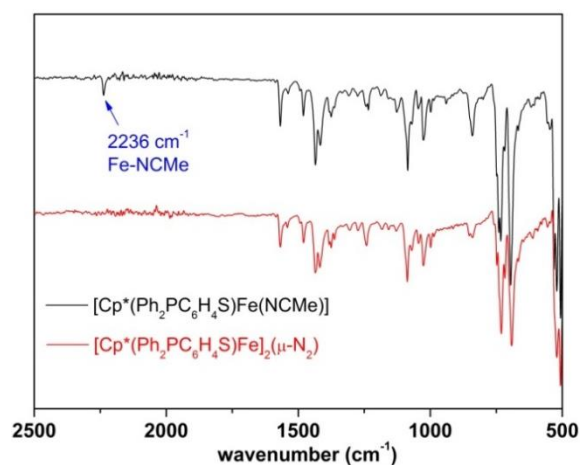


Figure S2. IR spectrum of $[\text{Cp}^*(\text{Ph}_2\text{PC}_6\text{H}_4\text{S})\text{Fe}(\text{NCMe})]$ and $[\text{Cp}^*(\text{Ph}_2\text{PC}_6\text{H}_4\text{S})\text{Fe}]_2(\mu\text{-N}_2)$.

2.2 Screening of reaction conditions

Table S1. Screening of reaction conditions in the hydroboration of pyridine^a

c1ccncc1 (2) + H-BR₂ $\xrightarrow[\text{C}_6\text{D}_6]{\text{1 (1 mol\%)}}$ c1cc[nH](BR2)c1 (3)

entry	borane <i>B-H</i>	T (°C)	time (h)	yield (%) ^b
1	BH ₃ ·THF	50	24	0
2	9-BBN	50	24	0
3	HBcat	50	24	0
4	HBpin	50	24	61
5 ^c	HBpin	50	24	46
6 ^d	HBpin	25	24	39
7 ^e	HBpin	50	36	0

^aReaction conditions: pyridine (0.24 mmol), borane (0.48 mmol, 2 equiv), **1** (1 mol%, 0.0024 mmol), tetraethylsilane (internal standard, 0.053 mmol) in 0.6 mL C₆D₆ unless otherwise noted. ^b¹H NMR yield based on pyridine. ^cIn the presence of 1 equiv of HBpin. ^dRoom temperature. ^eWithout **1**.

2.3 General procedures for the hydroboration of *N*-heteroarenes

NMR scale:

[Cp*(Ph₂PC₆H₄S)Fe]₂(μ-N₂) (2.4 mg, 0.0024 mmol), pyridine (19 mg, 0.24 mmol) and HBpin (62 mg, 0.48 mmol) were mixed in 0.6 mL C₆D₆ in a screw capped vial. Tetraethylsilane (10 μL, 0.053 mmol) was added as internal standard and the mixture was stirred at 50 °C for 24 h. Then the solution was transferred to a J. Young NMR tube and analyzed by ¹H NMR to determine the yield of the hydroborated product.

Preparative scale:

[Cp*(Ph₂PC₆H₄S)Fe]₂(μ-N₂) (18 mg, 0.018 mmol) and phenanthridine (322 mg, 1.8 mmol) and HBpin (461 mg, 3.6 mmol) were dissolved in 10 mL toluene in a flame-dried glassware in a glove box. The glassware was sealed with a septum, and stirred at room temperature for 24 h outside the glove box. Then the volatiles were removed in vacuo and the solid redissolved in hexane (5 mL). The solution was filtered through a short pad of celite, and the filtration was cooled at -30 °C to afford 5-(4,4,5,5-tetramethyl-1,3,2-dioxaborolan-2-yl)-5,6-dihydrophenanthridine (**5h**) as white solid (0.486 g, 88 % yield).

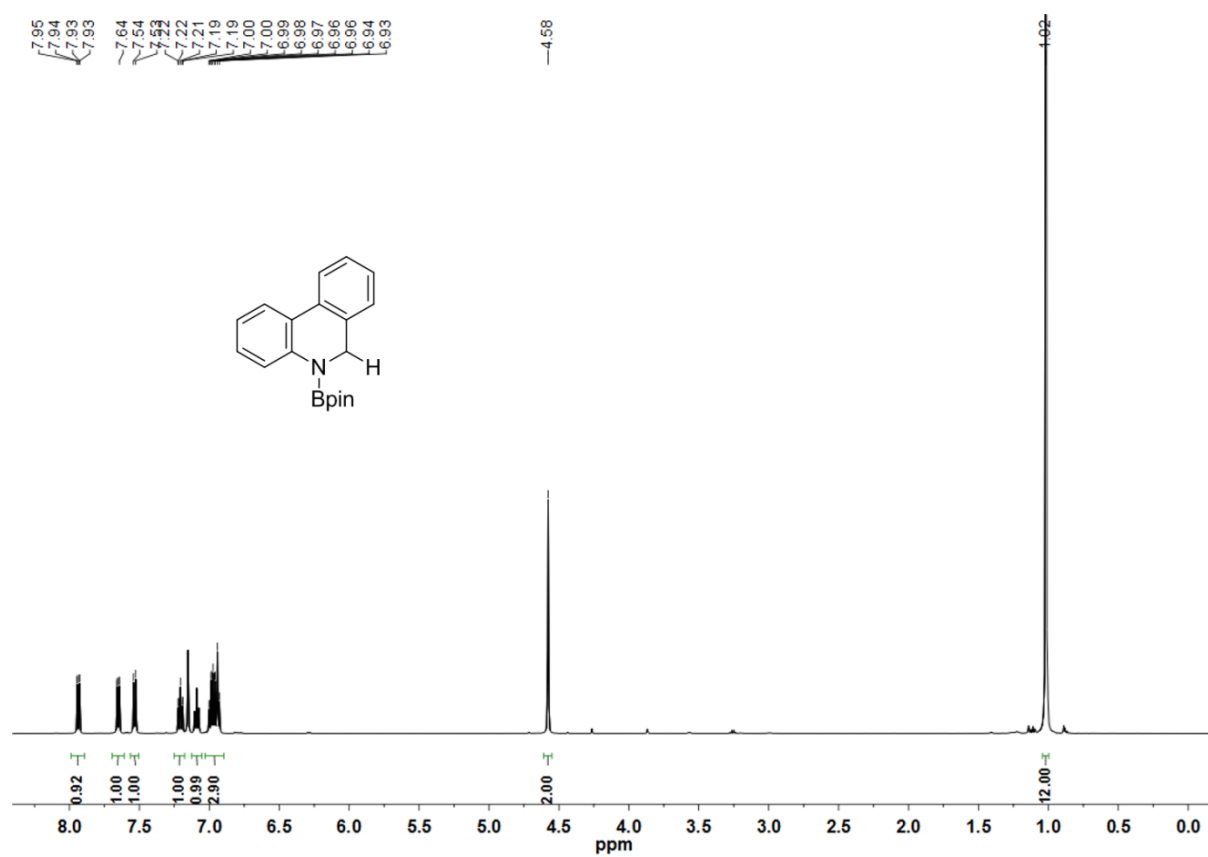


Figure S3. ¹H NMR spectrum of **5h** in C₆D₆.

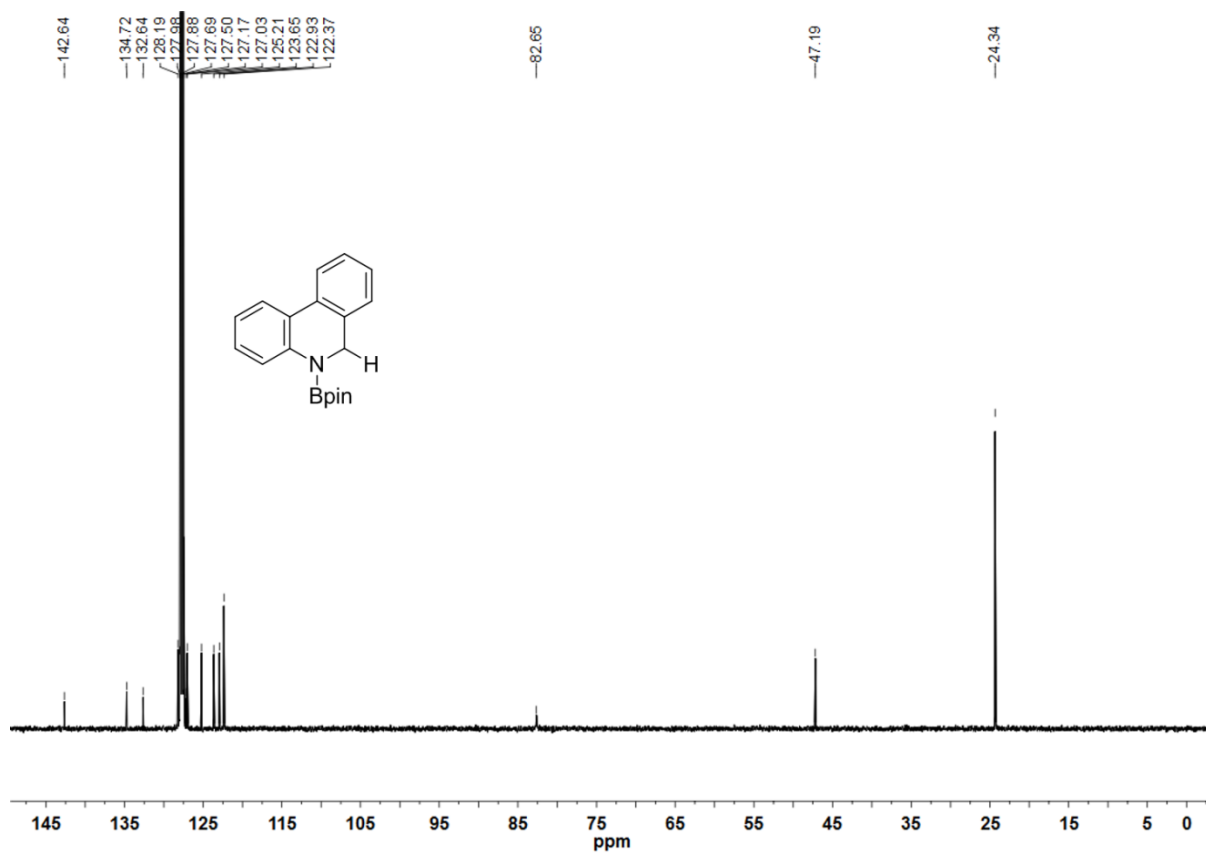


Figure S4. ^{13}C NMR spectrum of **5h** in C_6D_6 .

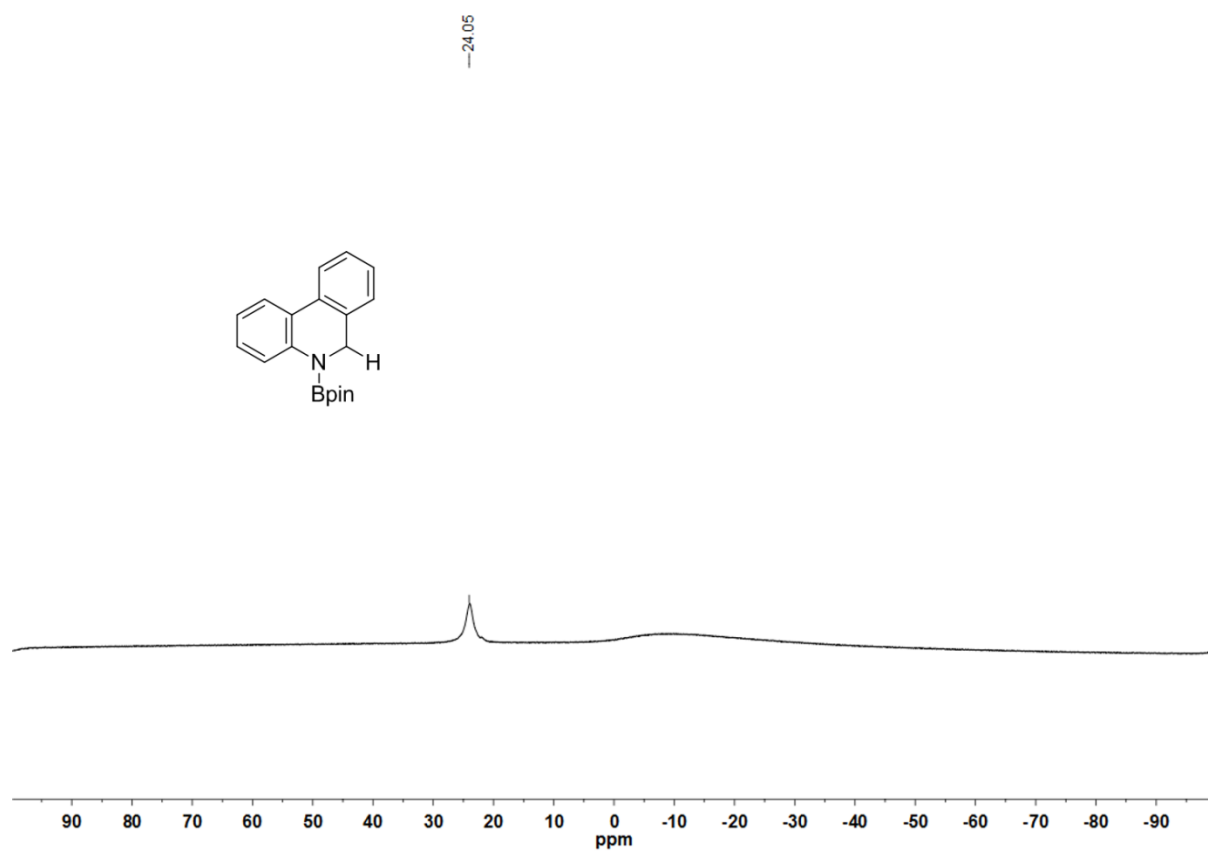
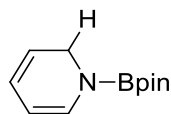
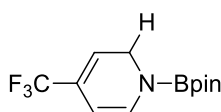


Figure S5. ^{11}B NMR spectrum of **5h** in C_6D_6 .

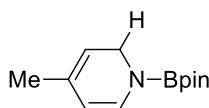
3. Characterization data of *N*-boryl-dihydropyridines

**3a**

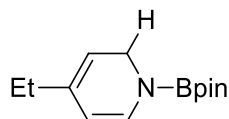
1-(4,4,5,5-Tetramethyl-1,3,2-dioxaborolan-2-yl)-1,2-dihydropyridine (3a).³ ¹H NMR (500 MHz, C₆D₆): δ 6.71 (d, J = 7.4 Hz, 1H), 5.80-5.77 (m, 1H), 5.11-5.06 (m, 2H), 4.15 (dd, J = 4.2, 1.6 Hz, 2H), 1.00 (s, 12H).

**3b**

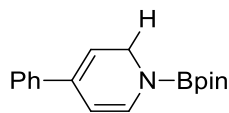
1-(4,4,5,5-tetramethyl-1,3,2-dioxaborolan-2-yl)-4-(trifluoromethyl)-1,2-dihydropyridine (3b).^{3b} ¹H NMR (500 MHz, C₆D₆): δ 6.59 (d, J = 7.6 Hz, 1H), 5.30-5.23 (m, 1H), 5.12 (dd, J = 7.6, 1.7 Hz, 1H), 3.89 (m, 2H), 0.99 (s, 12H).

**3c**

1-(4,4,5,5-tetramethyl-1,3,2-dioxaborolan-2-yl)-4-methyl-1,2-dihydropyridine (3c).³ ¹H NMR (500 MHz, C₆D₆): δ 6.70 (d, J = 7.4 Hz, 1H), 4.96 (dd, J = 7.5, 1.6 Hz, 1H), 4.85 (m, 1H), 4.16 (m, 2H), 1.57 (q, J = 1.5 Hz, 3H), 1.01 (s, 12H).

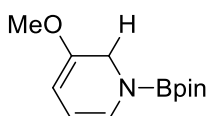
**3d**

1-(4,4,5,5-tetramethyl-1,3,2-dioxaborolan-2-yl)-4-ethyl-1,2-dihydropyridine (3d).^{3b} ¹H NMR (500 MHz, C₆D₆): δ 6.72 (d, J = 7.5 Hz, 1H), 5.00 (dd, J = 7.5, 1.6 Hz, 1H), 4.87 (m, 1H), 4.18 (m, 2H), 1.90 (qd, J = 7.4, 1.1 Hz, 2H), 1.01 (s, 12H), 0.93 (t, J = 7.5 Hz, 3H).

**3e**

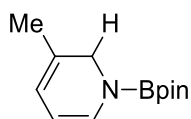
1-(4,4,5,5-Tetramethyl-1,3,2-dioxaborolan-2-yl)-4-phenyl-1,2-dihydropyridine (3e).^{3a, 3b}

¹H NMR (500 MHz, C₆D₆): δ 7.33-7.28 (m, 2H), 7.14-7.11 (m, 2H), 7.08-7.06 (m, 1H), 6.85 (dd, J = 7.6, 1.0 Hz, 1H), 5.51 (dd, J = 7.6, 1.8 Hz, 1H), 5.38-5.30 (m, 1H), 4.27 (d, J = 4.5 Hz, 2H), 1.03 (s, 12H).

**3f**

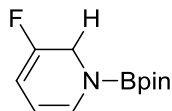
3-Methoxy-1-(4,4,5,5-tetramethyl-1,3,2-dioxaborolan-2-yl)-1,2-dihydropyridine (3f).^{3b}

¹H NMR (500 MHz, C₆D₆): δ 6.52 (d, J = 7.2 Hz, 1H), 5.12 (t, J = 6.6 Hz, 1H), 4.74 (d, J = 6.0 Hz, 1H), 4.33 (s, 2H), 3.12 (s, 3H), 1.00 (s, 12H).

**3g**

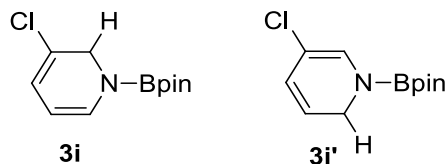
1-(4,4,5,5-Tetramethyl-1,3,2-dioxaborolan-2-yl)-3-methyl-1,2-dihydropyridine (3g).³

¹H NMR (500 MHz, C₆D₆): δ 6.61 (d, J = 7.4 Hz, 1H), 5.56-5.48 (m, 1H), 5.05 (dd, J = 7.3, 5.6 Hz, 1H), 4.09 (s, 2H), 1.42 (s, 3H), 1.03 (s, 12H).

**3h**

1-(4,4,5,5-tetramethyl-1,3,2-dioxaborolan-2-yl)-3-fluoro-1,2-dihydropyridine (3h).^{3b}

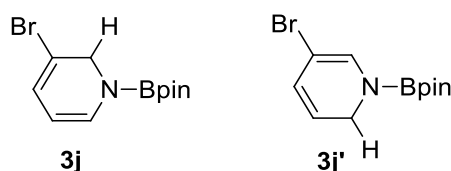
¹H NMR (500 MHz, C₆D₆): δ 6.37 (dd, J = 7.3, 1.8 Hz, 1H), 5.30 (dd, J = 12.0, 6.3 Hz, 1H), 4.71 (dt, J = 7.2, 6.0 Hz, 1H), 4.28 (t, J = 1.5 Hz, 2H), 0.99 (s, 12H).



1-(4,4,5,5-tetramethyl-1,3,2-dioxaborolan-2-yl)-3-chloro-1,2-dihydropyridine (3i) and 1-(4,4,5,5-tetramethyl-1,3,2-dioxaborolan-2-yl)-5-chloro-1,2-dihydropyridine (3i').⁴

3i: ¹H NMR (500 MHz, C₆D₆): δ 6.49 (d, J = 7.3 Hz, 1H), 5.79 (d, J = 6.0 Hz, 1H), 4.76 (dd, J = 7.2, 6.1 Hz, 1H), 4.31 (d, J = 1.3 Hz, 2H), 0.96 (s, 12H).

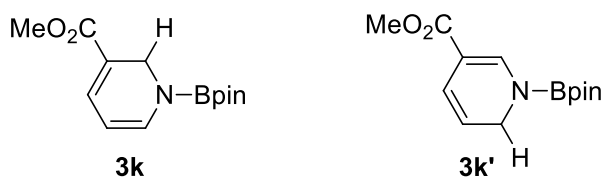
3i': ¹H NMR (500 MHz, C₆D₆): δ 6.78 (s, 1H), 5.75 (ddd, J = 9.8, 3.3, 1.6 Hz, 1H), 4.93-4.87 (m, 1H), 3.88 (dd, J = 4.3, 1.7 Hz, 2H), 0.97 (s, 12H).



1-(4,4,5,5-tetramethyl-1,3,2-dioxaborolan-2-yl)-3-bromo-1,2-dihydropyridine (3j) and 1-(4,4,5,5-tetramethyl-1,3,2-dioxaborolan-2-yl)-5-bromo-1,2-dihydropyridine (3j').⁴

3j: ¹H NMR (500 MHz, C₆D₆): δ 6.54 (d, J = 7.2 Hz, 1H), 6.00 (d, J = 6.0 Hz, 1H), 4.72 (dd, J = 7.1, 6.2 Hz, 1H), 4.39 (d, J = 1.2 Hz, 2H), 0.95 (s, 12H).

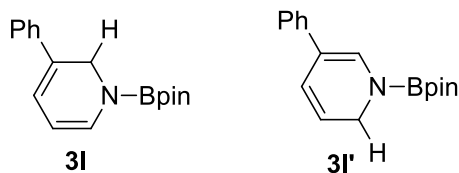
3j': ¹H NMR (500 MHz, C₆D₆): δ 6.89 (s, 1H), 5.82 (dd, J = 9.8, 1.4 Hz, 1H), 4.90-4.82 (m, 1H), 3.91-3.86 (m, 2H), 0.97 (s, 12H).



Methyl 1-(4,4,5,5-tetramethyl-1,3,2-dioxaborolan-2-yl)-1,2-dihydropyridine-3-carboxylate (3k) and Methyl 1-(4,4,5,5-tetramethyl-1,3,2-dioxaborolan-2-yl)-1,2-dihydropyridine-5-carboxylate (3k').^{3a, 3b} **3k:** ¹H NMR (500 MHz, C₆D₆): δ 7.06 (d, J = 5.9 Hz, 1H), 6.80 (d, J = 7.1 Hz, 1H), 5.01-4.98 (m, 1H), 4.54 (s, 2H), 3.37 (s, 3H), 0.96 (s, 12H).

3k': ¹H NMR (500 MHz, C₆D₆): δ 7.89 (s, 1H), 6.61 (dd, J = 10.0, 1.4 Hz, 1H), 4.94 (dt, J =

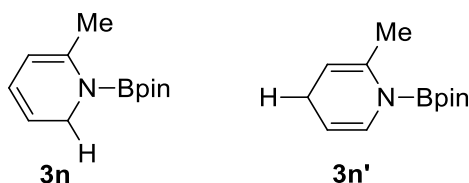
9.2, 3.7 Hz, 1H), 4.00 (dd, $J = 3.7, 1.8$ Hz, 2H), 3.43 (s, 3H), 0.94 (s, 12H).



1-(4,4,5,5-tetramethyl-1,3,2-dioxaborolan-2-yl)-3-phenyl-1,2-dihydropyridine (3l) and 1-(4,4,5,5-tetramethyl-1,3,2-dioxaborolan-2-yl)-5-phenyl-1,2-dihydropyridine (3l').⁴ 3l:

¹H NMR (500 MHz, C₆D₆): δ 7.28-6.98 (m, 5H), 6.81 (d, $J = 7.2$ Hz, 1H), 6.28 (d, $J = 5.9$ Hz, 1H), 5.25-5.22 (m, 2H), 4.61 (d, $J = 0.9$ Hz, 2H), 1.01 (s, 12H).

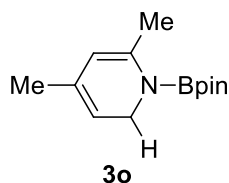
3l': ¹H NMR (500 MHz, C₆D₆): δ 7.28-6.98 (m, 5H), 7.12 (s, 1H), 6.32 (dd, $J = 9.7, 1.5$ Hz, 1H), 5.25-5.22 (m, 2H), 4.14 (dd, $J = 4.2, 1.7$ Hz, 2H), 1.03 (s, 12H).



1-(4,4,5,5-Tetramethyl-1,3,2-dioxaborolan-2-yl)-6-methyl-1,2-dihydropyridine (3n) and 1-(4,4,5,5-Tetramethyl-1,3,2-dioxaborolan-2-yl)-2-methyl-1,4-dihydropyridine (3n').³ 3n:

¹H NMR (500 MHz, C₆D₆): δ 5.89 (dd, $J = 9.1, 5.2$ Hz, 1H), 5.28 (dt, $J = 9.0, 4.4$ Hz, 1H), 5.21 (dd, $J = 4.2, 1.0$ Hz, 1H), 4.10 (dd, $J = 4.4, 1.1$ Hz, 2H), 2.18 (s, 3H), 1.00 (s, 12H).

3n': ¹H NMR (500 MHz, C₆D₆): δ 6.76 (dt, $J = 8.2, 1.5$ Hz, 1H), 4.73-4.67 (m, 1H), 4.47 (m, 1H), 2.83 (dq, $J = 5.0, 1.6$ Hz, 2H), 2.06 (s, 3H), 0.97 (s, 12H).

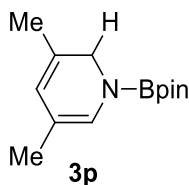


1-(4,4,5,5-Tetramethyl-1,3,2-dioxaborolan-2-yl)-2,4-dimethyl-1,2-dihydropyridine (3o).

¹H NMR (500 MHz, C₆D₆): δ 5.09 (s, 1H), 5.02 (s, 1H), 4.10 (dd, $J = 4.2, 1.3$ Hz, 2H), 2.19 (s, 3H), 1.63 (s, 3H), 1.01 (s, 12H).

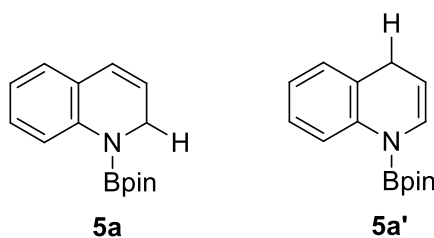
¹³C NMR (126 M, C₆D₆): δ 141.6, 132.8, 109.9, 109.7, 82.1, 44.2, 24.3, 21.4, 19.9.

¹¹B NMR (160 M, C₆D₆): δ 23.6.



1-(4,4,5,5-Tetramethyl-1,3,2-dioxaborolan-2-yl)-3,5-dimethyl-1,2-dihydropyridine (3p).³

¹H NMR (500 MHz, C₆D₆): δ 6.43 (s, 1H), 5.44 (s, 1H), 4.04 (s, 2H), 1.63 (s, 3H), 1.46 (s, 3H), 1.05 (s, 12H).

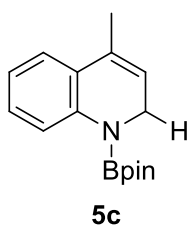


1-(4,4,5,5-tetramethyl-1,3,2-dioxaborolan-2-yl)-1,2-dihydroquinoline (5a) and

1-(4,4,5,5-tetramethyl-1,3,2-dioxaborolan-2-yl)-1,2-dihydroquinoline (5a').^{3a, 3c} **5a:** ¹H

NMR (500 MHz, C₆D₆): δ 7.79 (d, J = 8.1 Hz, 1H), 7.14-7.05 (m, 1H), 6.93-6.77 (m, 2H), 6.25 (d, J = 9.5 Hz, 1H), 5.61-5.52 (m, 1H), 4.14 (dd, J = 4.0, 1.3 Hz, 2H), 1.04 (s, 12H).

5a': ¹H NMR (500 MHz, C₆D₆): δ 8.14 (d, J = 8.3 Hz, 1H), 7.13-7.04 (m, 1H), 6.94-6.76 (m, 3H), 4.88-4.75 (m, 1H), 3.31 (d, J = 2.4 Hz, 2H), 1.01 (s, 12H).

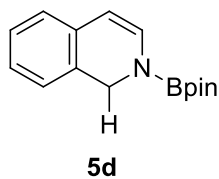


1-(4,4,5,5-tetramethyl-1,3,2-dioxaborolan-2-yl)-4-methyl-1,2-dihydroquinoline (5c). ¹H

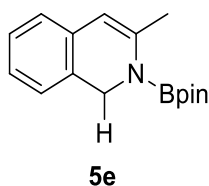
NMR (500 MHz, C₆D₆): δ 7.80 (d, J = 8.1 Hz, 1H), 7.14-7.09 (m, 1H), 7.07 (dd, J = 7.6, 1.2 Hz, 1H), 6.86 (td, J = 7.6, 0.9 Hz, 1H), 5.46-5.40 (m, 1H), 4.11 (dd, J = 4.1, 1.5 Hz, 2H), 1.80 (s, J = 1.4 Hz, 3H), 1.05 (s, 12H).

¹³C NMR (126 M, C₆D₆): δ 142.0, 131.2, 128.5, 127.6, 123.4, 121.4, 121.3, 121.0, 82.4, 43.1, 24.4, 18.4.

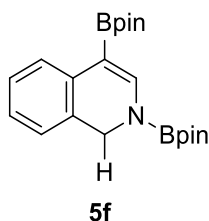
¹¹B NMR (160 M, C₆D₆): δ 23.9.



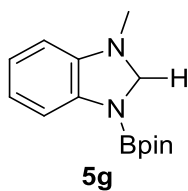
1-(4,4,5,5-tetramethyl-1,3,2-dioxaborolan-2-yl)-1,2-dihydroisoquinoline (5d).^{3a, 3c} ¹H NMR (500 MHz, C₆D₆): δ 6.99 (t, J = 7.4 Hz, 1H), 6.88 (td, J = 7.4, 0.8 Hz, 1H), 6.81 (t, J = 8.3 Hz, 2H), 6.72 (d, J = 7.4 Hz, 1H), 5.62 (d, J = 7.5 Hz, 1H), 4.62 (s, 2H), 1.02 (s, 12H).



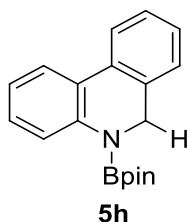
1-(4,4,5,5-tetramethyl-1,3,2-dioxaborolan-2-yl)-3-methyl-1,2-dihydroisoquinoline (5e). ¹H NMR (500 MHz, C₆D₆): δ 7.04 (t, J = 7.3 Hz, 1H), 6.92 (t, J = 7.3 Hz, 1H), 6.87 (d, J = 7.6 Hz, 2H), 5.71 (s, 1H), 4.61 (s, 2H), 2.24 (s, 3H), 1.00 (s, 12H). ¹³C NMR (126 MHz, C₆D₆): δ 142.7, 134.4, 129.5, 127.1, 125.2, 124.4, 122.5, 108.4, 82.4, 48.1, 24.3, 21.6. ¹¹B NMR (160 MHz, C₆D₆): δ 23.4.



1-(4,4,5,5-tetramethyl-1,3,2-dioxaborolan-2-yl)-4-(4,4,5,5-tetramethyl-1,3,2-dioxaborolan-2-yl)-1,2-dihydroisoquinoline (5f). ¹H NMR (500 MHz, C₆D₆): δ 8.29 (d, J = 7.6 Hz, 1H), 7.88 (s, 1H), 7.17 (t, J = 7.9 Hz, 1H), 6.93 (t, J = 7.2 Hz, 1H), 6.75 (d, J = 7.3 Hz, 1H), 4.60 (s, 2H), 1.09 (s, 12H), 0.97 (s, 12H). ¹³C NMR (126 MHz, C₆D₆): δ 146.3, 134.6, 128.1, 127.4, 125.53, 125.46, 125.0, 83.3, 82.4, 46.1, 24.6, 24.3. ¹¹B NMR (160 MHz, C₆D₆): δ 31.4, 24.2.

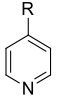
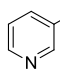
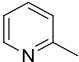
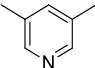
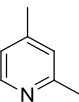
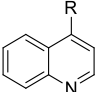
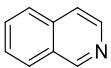
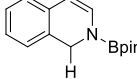
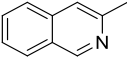
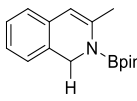
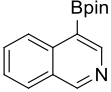
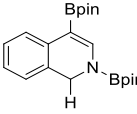
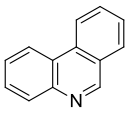
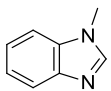
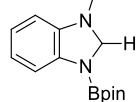


1-(4,4,5,5-tetramethyl-1,3,2-dioxaborolan-2-yl)-3-methyl-2,3-dihydro-1H-benzo[d]imidazole (5g). ^1H NMR (500 MHz, C_6D_6): δ 7.47 (dd, $J = 7.4, 1.2$ Hz, 1H), 6.78 (dtd, $J = 21.4, 7.6, 1.2$ Hz, 2H), 6.30 (dd, $J = 7.3, 0.9$ Hz, 1H), 4.74 (s, 2H), 2.24 (s, 3H), 1.07 (s, 12H). ^{13}C NMR (126 MHz, C_6D_6): δ 144.2, 138.0, 121.0, 118.8, 111.4, 106.1, 82.5, 72.5, 33.5, 24.4. ^{11}B NMR (160 MHz, C_6D_6): δ 23.3.



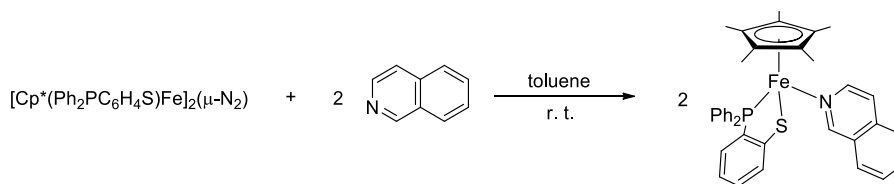
5-(4,4,5,5-tetramethyl-1,3,2-dioxaborolan-2-yl)-5,6-dihydrophenanthridine (5h). ^1H NMR (500 MHz, C_6D_6): δ 7.89 (d, $J = 8.1$ Hz, 1H), 7.64 (d, $J = 7.6$ Hz, 1H), 7.52 (d, $J = 7.7$ Hz, 1H), 7.19 (t, $J = 7.6$ Hz, 1H), 7.09 (t, $J = 7.4$ Hz, 1H), 7.01-6.90 (m, 3H), 4.55 (s, 2H), 1.02 (s, 12H). ^{13}C NMR (126 MHz, C_6D_6): δ 142.6, 134.7, 132.6, 128.2, 127.1, 127.0, 125.2, 123.6, 122.9, 122.3, 82.6, 47.2, 24.4. ^{11}B NMR (160 MHz, C_6D_6): δ 24.0.

4. Reactions of *N*-heteroarenes with HBpin without compound 1Table S2. Reaction of *N*-heteroarenes with HBpin without 1^a

entry	pyridines	conversion (%)	product
1	 R = H, CF ₃ , Me, Et, Ph	Not observed	-
2	 R = F, Cl, Br, OMe, CH ₃ , CO ₂ Me, Ph	Not observed	-
3		Not observed	-
4		Not observed	-
5		Not observed	-
6	 R = H, Me	< 5	-
7		10	
8		< 5	
9		32	
10		Not observed	-
11		16	

^aThe mixture of *N*-heteroarene (0.24 mmol) and HBpin (0.48 mmol) in C₆D₆ was stirred at 50 °C for 24 h.^bConversion was determined via ¹H NMR analysis.

5. Reaction of $[\text{Cp}^*(\text{Ph}_2\text{PC}_6\text{H}_4\text{S})\text{Fe}]_2(\mu\text{-N}_2)$ with isoquinoline and pyridines.



$[\text{Cp}^*(\text{Ph}_2\text{PC}_6\text{H}_4\text{S})\text{Fe}(\text{C}_9\text{H}_9\text{N})]$, 6. $[\text{Cp}^*(\text{Ph}_2\text{PC}_6\text{H}_4\text{S})\text{Fe}]_2(\mu\text{-N}_2)$ (50 mg, 0.05 mmol) was dissolved in 3 mL of toluene in a vial under nitrogen in glovebox. To this solution isoquinoline (14 μL , 0.12 mmol) was added, and the resulted mixture was stirred at room temperature for 10 min, the color turned to black immediately. Hexane was layered on top of the solution and the mixture was stored at -30°C to provide $[\text{Cp}^*(\text{Ph}_2\text{PC}_6\text{H}_4\text{S})\text{Fe}(\text{C}_9\text{H}_9\text{N})]$ (**6**) as black crystals (47 mg, yield 76%). Anal. Calcd for $\text{C}_{37}\text{H}_{36}\text{FeNPS}$: 72.43; H, 5.92; N, 2.28. Found: C, 72.62; H, 5.75; N, 2.19. ESI-MS calcd. for $[\text{Cp}^*(\text{Ph}_2\text{PC}_6\text{H}_4\text{S})\text{Fe}]$, 484.1077; found, 484.1063. Magnetic susceptibility (μ_{eff} , C_6D_6 , 23°C): $2.92 \mu_{\text{B}}$.

$[\text{Cp}^*(\text{Ph}_2\text{PC}_6\text{H}_4\text{S})\text{Fe}(\text{C}_5\text{H}_5\text{N})]$, 7. Complex **7** was synthesized using the same procedure as described for **6** using $[\text{Cp}^*(\text{Ph}_2\text{PC}_6\text{H}_4\text{S})\text{Fe}]_2(\mu\text{-N}_2)$ and pyridine. The product was isolated as deep-red crystals (41 mg, yield 73%). Anal. Calcd for $\text{C}_{33}\text{H}_{34}\text{FeNPS}$: C, 70.35; H, 6.09; N, 2.48. Found: C, 70.46; H, 6.31; N, 2.73. Magnetic susceptibility (μ_{eff} , C_6D_6 , 23°C): $2.83 \mu_{\text{B}}$.

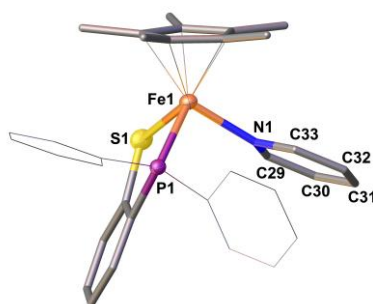


Figure S6. Crystal structure of **7** (50% probability thermal ellipsoids).

[Cp*(Ph₂PC₆H₄S)Fe(C₆H₇N)], 8. Complex **8** was synthesized using the same procedure as described for **6** using [Cp*(Ph₂PC₆H₄S)Fe]₂(μ-N₂) and 2-methylpyridine. The product was isolated as red crystals (39 mg, yield 68%). Anal. Calcd for C₃₄H₃₆FeNPS: C, 70.72; H, 6.29; N, 2.42. Found: C, 70.81; H, 6.43; N, 2.57. Magnetic susceptibility (μ_{eff}, C₆D₆, 23 °C): 2.97 μ_B.

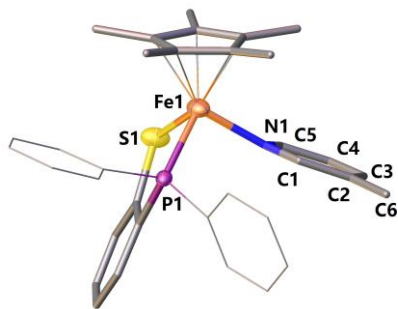


Figure S7. Crystal structure of **8** (50% probability thermal ellipsoids).

6. X-ray crystal structure determinations

Crystals of $[\text{Cp}^*(\text{Ph}_2\text{PC}_6\text{H}_4\text{S})\text{Fe}]_2(\mu\text{-N}_2)$ (**1**) and $[\text{Cp}^*(\text{Ph}_2\text{PC}_6\text{H}_4\text{S})\text{Fe}(\text{C}_5\text{H}_5\text{N})]$ (**7**) were obtained by recrystallization from toluene/hexane at $-30\text{ }^\circ\text{C}$. Crystals of $[\text{Cp}^*(\text{Ph}_2\text{PC}_6\text{H}_4\text{S})\text{Fe}(\text{C}_9\text{H}_7\text{N})]$ (**6**) and $[\text{Cp}^*(\text{Ph}_2\text{PC}_6\text{H}_4\text{S})\text{Fe}(\text{C}_6\text{H}_7\text{N})]$ (**8**) were obtained by slow evaporation of a diethyl ether solution. Crystals of **5 h** was obtained from saturated hexane solution at $-30\text{ }^\circ\text{C}$. Single crystals were coated with inert oil, placed under streaming nitrogen in a Bruker Apex II CCD diffractometer (Mo $\text{K}\alpha$ radiation, $\lambda = 0.71073\text{ \AA}$) for **1** and **7**. Rigaku Oxford Diffraction XtaLAB Synergy diffractometer equipped with a HyPix-6000HE area detector (Cu $\text{K}\alpha$ radiation, $\lambda = 1.54184\text{ \AA}$) for **5h**, **6** and **8**. The structure was solved using the charge-flipping algorithm, as implemented in the program *SUPERFLIP*⁵ and refined by full-matrix least-squares techniques against F_o^2 using the SHELXL program⁶ through the OLEX2 interface.⁷ Hydrogen atoms bonded to carbon were placed at calculated positions and refined isotropically by using a riding model. Both structures were examined using the Addsym subroutine of PLATON⁸ to ensure that no additional symmetry could be applied to the models. Crystallographic and experimental details of the structure determination are summarized in Table S3. CCDC 1581384-1581387 contain the supplementary crystallographic data for **1**, **5h**, **6**, **7** and 1587262 for **8**. These data are provided free of charge by The Cambridge Crystallographic Data Centre.

7. Iron-catalyzed hydroboration of 2-methylpyridine with HBpin

Table S3. Product ratios for the Iron-catalyzed hydroboration of 2-methylpyridine^a

entry	Time (h)	yield (%) ^b	product ratio (3n:3n')
1	4	10	65:35
2	8	17	64:36
3	20	34	64:36
4	32	45	65:35
5	48	60	65:35

^aReaction conditions: 2-methylpyridine (0.24 mmol), HBpin (0.48 mmol, 2 equiv), **1** (2.5 mol%, 0.006 mmol), tetraethylsilane (internal standard, 0.053 mmol) in 0.6 mL C₆D₆. ^b¹H NMR yield.

Table S4. Product ratios for the Iron-catalyzed hydroboration of 2-methylpyridine with different concentration of **1**^a

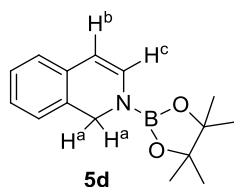
entry	[1] (mol%)	yield (%) ^b	product ratio (3n:3n')
1	0.5	11	64:36
2	1	23	64:36
3	4	67	67:33
4	8	88	65:35

^aReaction conditions: 2-methylpyridine (0.24 mmol), HBpin (0.48 mmol, 2 equiv), tetraethylsilane (internal standard, 0.053 mmol) in 0.6 mL C₆D₆ in 24 h. ^b¹H NMR yield.

8. Stoichiometric reaction of $[\text{Cp}^*(\text{Ph}_2\text{PC}_6\text{H}_4\text{S})\text{Fe}(\text{C}_9\text{H}_7\text{N})]$ (**6**) with HBpin

8.1 Reaction of $[\text{Cp}^*(\text{Ph}_2\text{PC}_6\text{H}_4\text{S})\text{Fe}(\text{C}_9\text{H}_7\text{N})]$ with HBpin

$[\text{Cp}^*(\text{Ph}_2\text{PC}_6\text{H}_4\text{S})\text{Fe}(\text{C}_9\text{H}_7\text{N})]$ (20 mg, 0.032 mmol) and tetraethylsilane (internal standard) (0.009 mmol) were dissolved in C_6D_6 (0.5 mL) in a vial. HBpin (4.2 mg, 0.032 mmol) was added and the resulting mixture was stirred at room temperature for 10 min. It was transferred to a J. Young NMR tube and analyzed by ^1H NMR. **5d** was formed in 93 % yield according to ^1H NMR analysis of the crude reaction mixture.



^1H NMR (500 MHz, C_6D_6): δ 6.99 (t, $J = 7.3$ Hz, 1H, ArCH), 6.89 (t, $J = 7.4$ Hz, 1H, ArCH), 6.84 (d, $J = 7.5$ Hz, 1H), 6.81 (d, $J = 7.4$ Hz, 1H, H^c), 6.73 (d, $J = 7.4$ Hz, 1H, ArCH), 5.63 (d, $J = 7.5$ Hz, 1H, H^b), 4.64 (s, 2H, H^a), 1.03 (s, 12H, CH_3).

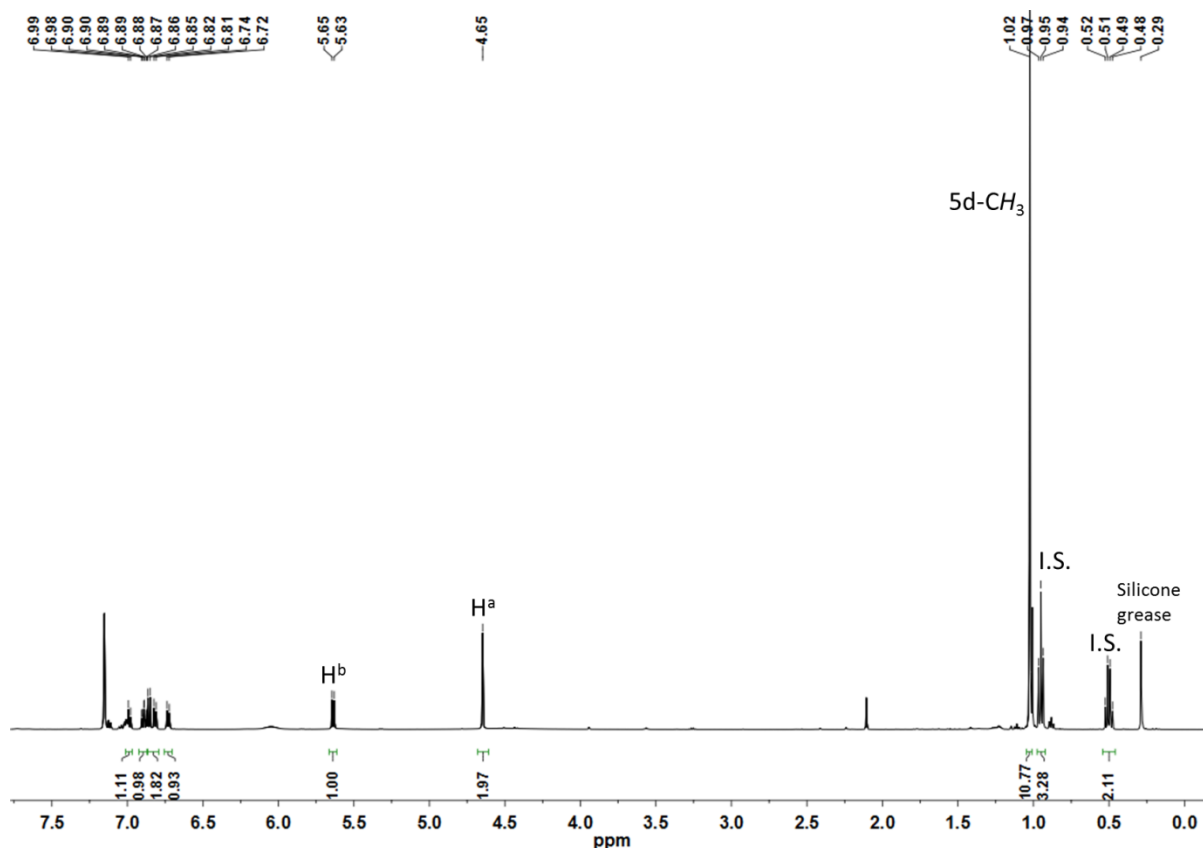
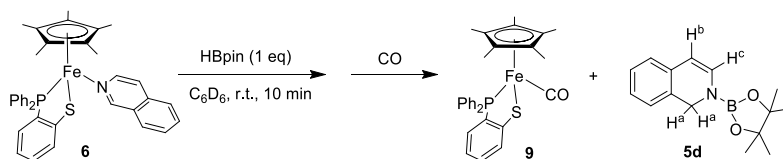


Figure S8. ^1H NMR for the reaction of $[\text{Cp}^*(\text{Ph}_2\text{PC}_6\text{H}_4\text{S})\text{Fe}(\text{C}_9\text{H}_7\text{N})]$ with HBpin in C_6D_6 . I.S. = internal standard.

8.2 Reaction of $[\text{Cp}^*(\text{Ph}_2\text{PC}_6\text{H}_4\text{S})\text{Fe}(\text{C}_9\text{H}_7\text{N})]$ with HBpin and CO



$[\text{Cp}^*(\text{Ph}_2\text{PC}_6\text{H}_4\text{S})\text{Fe}(\text{C}_9\text{H}_7\text{N})]$ (20 mg, 0.032 mmol) and tetraethylsilane (internal standard) (0.015 mmol) were dissolved in C_6D_6 (0.5 mL) in a Schlenk tube. HBpin (4.2 mg, 0.032 mmol) was added and the resulting mixture was stirred at room temperature for 10 min. Then CO was bubbled through the solution for 1 min, during which time the color turned to red. The solution was transferred to a J. Young NMR tube and analyzed by ^1H NMR.⁹ The yield of **5d** was 91% according to NMR analysis.

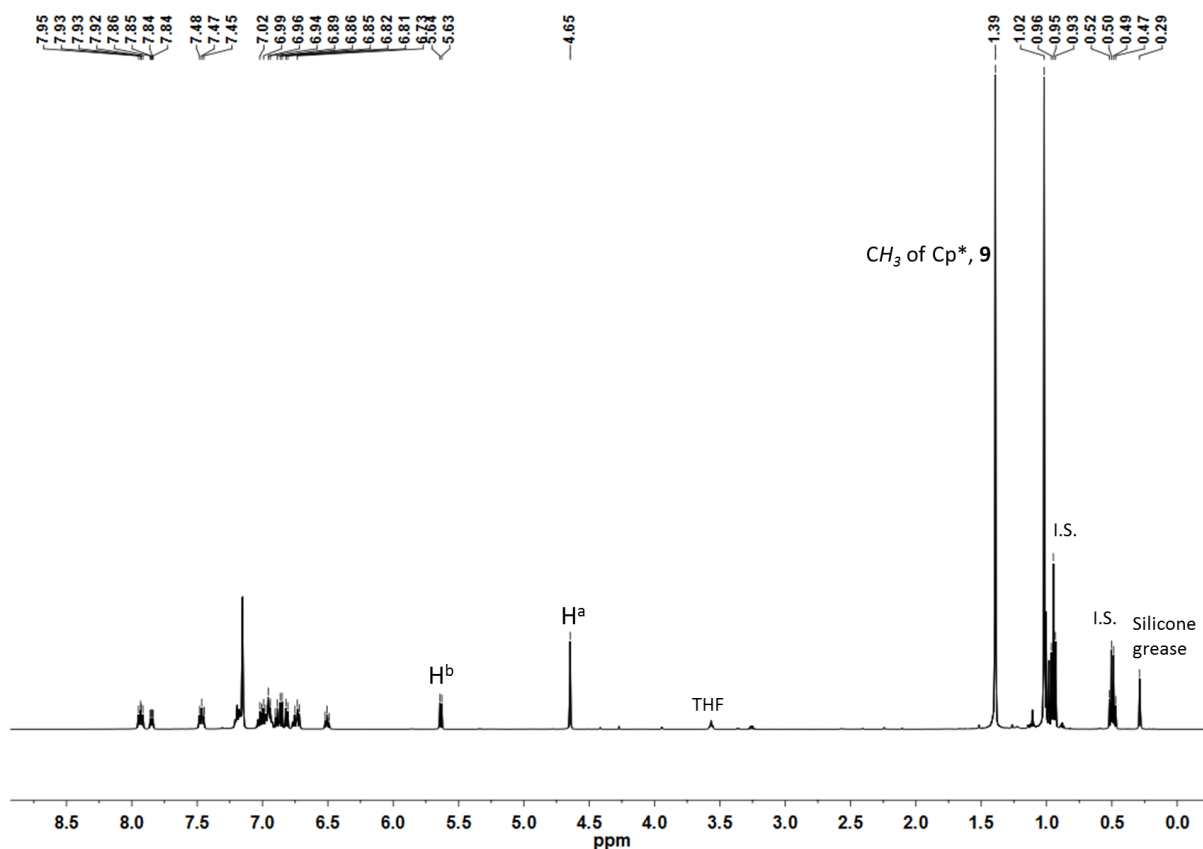


Figure S9. ^1H NMR for the reaction of $[\text{Cp}^*(\text{Ph}_2\text{PC}_6\text{H}_4\text{S})\text{Fe}(\text{C}_9\text{H}_7\text{N})]$ with HBpin and CO in C_6D_6 .

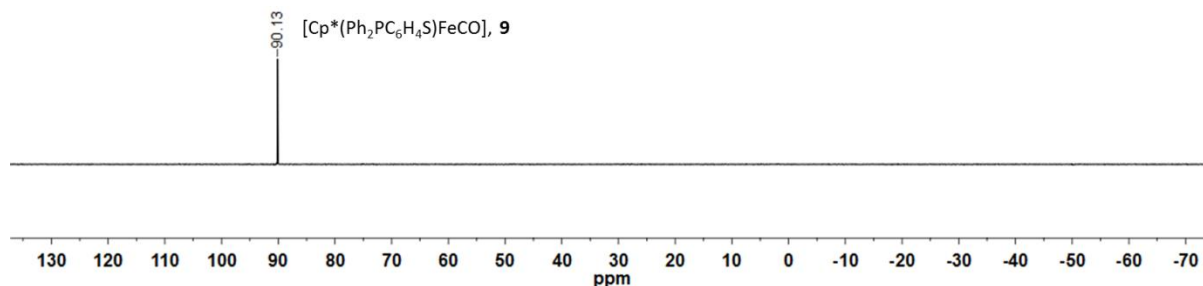
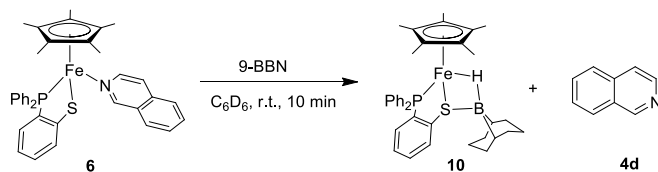
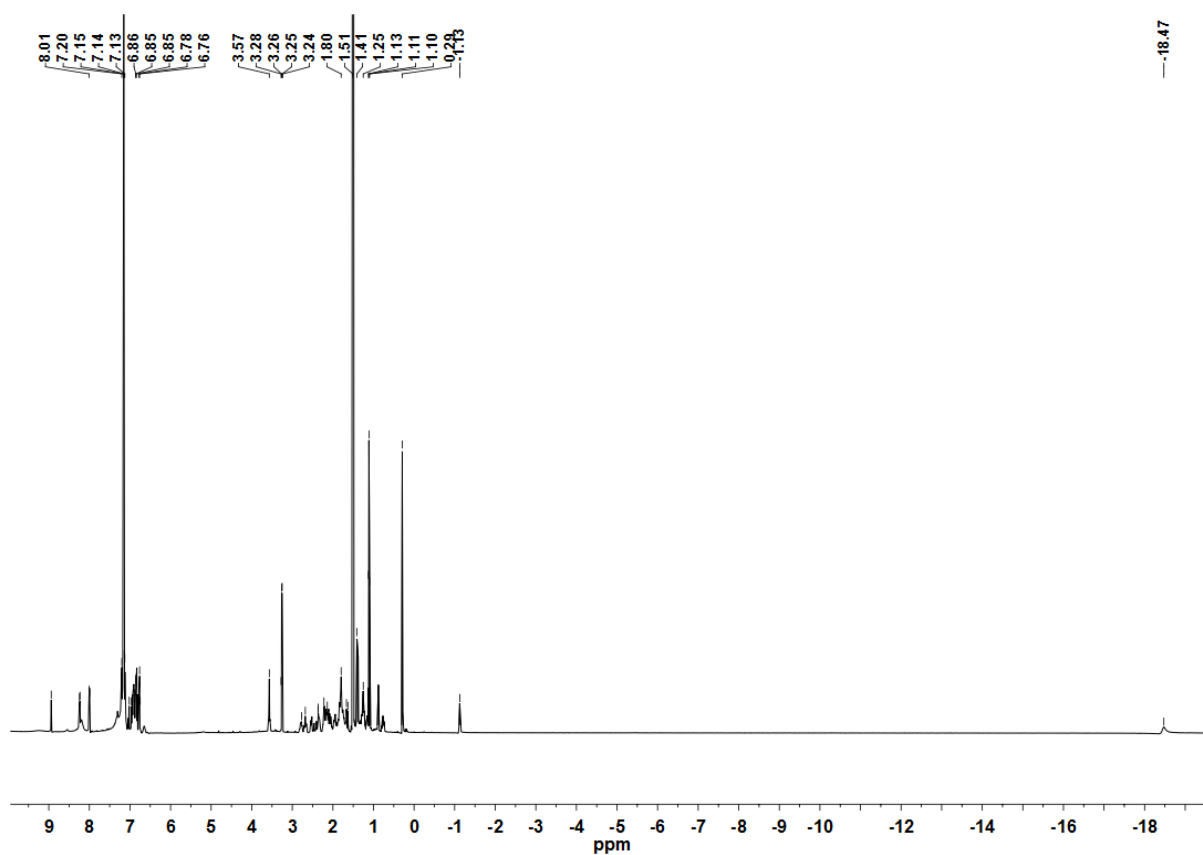


Figure S10. ^{31}P NMR for the reaction of $[\text{Cp}^*(\text{Ph}_2\text{PC}_6\text{H}_4\text{S})\text{Fe}(\text{C}_9\text{H}_7\text{N})]$ with HBpin and CO in C_6D_6 .

8.3 Reaction of $[\text{Cp}^*(\text{Ph}_2\text{PC}_6\text{H}_4\text{S})\text{Fe}(\text{C}_9\text{H}_7\text{N})]$ with 9-BBN



$[\text{Cp}^*(\text{Ph}_2\text{PC}_6\text{H}_4\text{S})\text{Fe}(\text{C}_9\text{H}_7\text{N})]$ (20 mg, 0.032 mmol) was dissolved in C_6D_6 (0.5 mL) in a vial. 9-BBN (0.033 mmol, 0.5 mol/L in THF, THF was removed under vacuum before use) was added, and the color turned to red-brown. The resulting mixture was stirred at room temperature for 10 min, then it was transferred to a J. Young NMR tube and analyzed by ^1H NMR.⁹



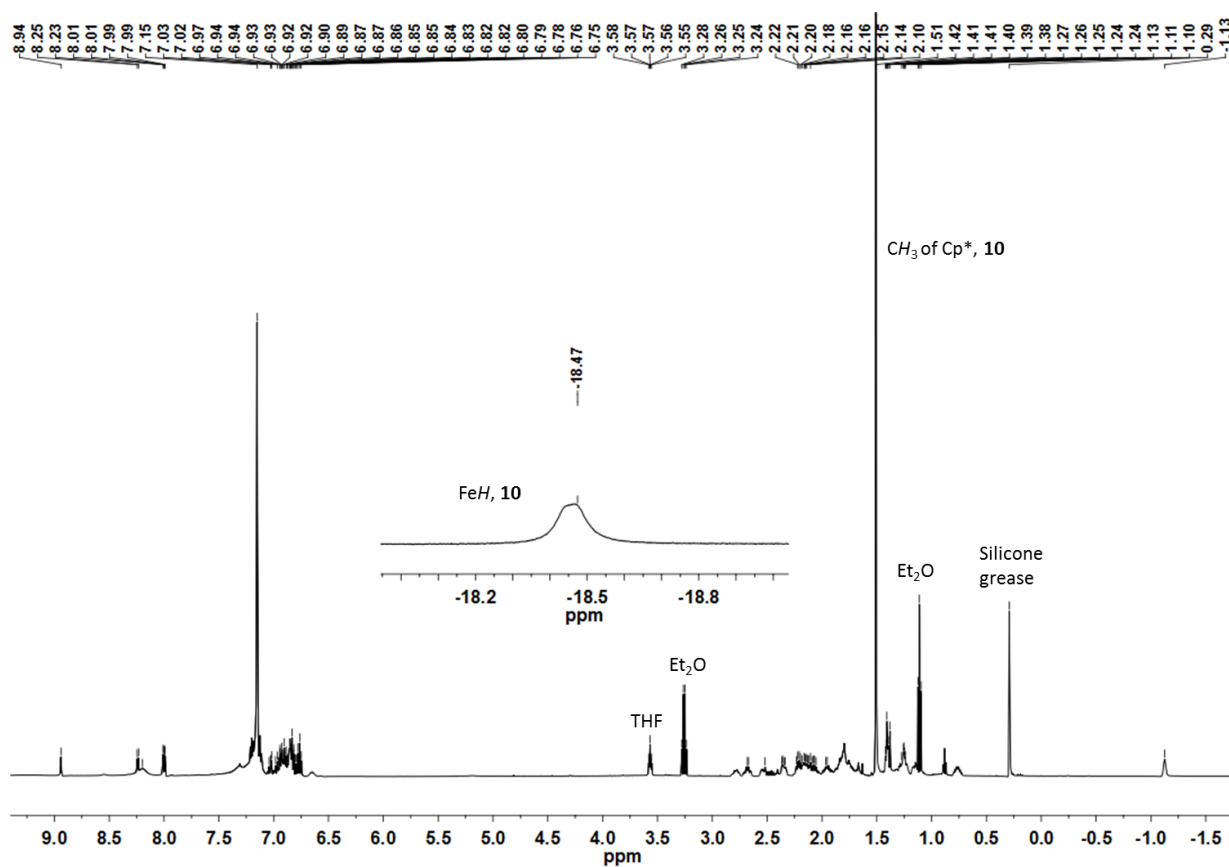


Figure S11. ^1H NMR for the reaction of $[\text{Cp}^*(\text{Ph}_2\text{PC}_6\text{H}_4\text{S})\text{Fe}(\text{C}_9\text{H}_7\text{N})]$ with 9-BBN in C_6D_6 .

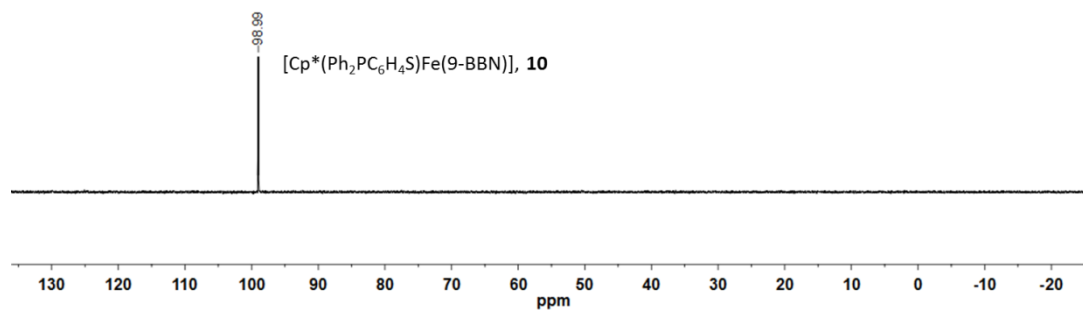


Figure S12. ^{31}P NMR for the reaction of $[\text{Cp}^*(\text{Ph}_2\text{PC}_6\text{H}_4\text{S})\text{Fe}(\text{C}_9\text{H}_7\text{N})]$ with 9-BBN in C_6D_6 .

9. Kinetic experiments

Kinetic analysis of the NMR scale reaction was carried out by collecting multiple (10~20) data points early in the reaction before the substrate concentrations were depleted. Under these conditions, the reaction can be approximated as pseudo-zero-order with respect to the substrate concentrations. The reaction was monitored by ^1H NMR (500 MHz, C_6D_6) analysis at 60 s intervals over 2 h at 298.1 K. The kinetic data were obtained from intensity increase in the C3-*H* integral of dearomatized 1,2-dihydroisoquinoline over time (up to 20% conversion) relative to tetraethylsilane (internal standard) to determine the initial reaction rate. Data were fit by least-squares analysis ($R^2 > 0.98$).

General procedure for initial rate

200 μL of a solution of compound **1** (C_6D_6 , 0.01 M, 2 μmol) and tetraethylsilane (5 μL , 26 μmol) were added to a J. Young NMR tube in a glovebox. Then isoquinoline (24 μL , 0.2 mmol) and 340 μL C_6D_6 were added and the NMR tube of the resulting solution was put in a pre-cooled bath at $-30\text{ }^\circ\text{C}$ under N_2 atmosphere. After 10 min, HBpin (35 μL , 0.24 mmol, 1.2 equiv) was added to the solution while maintaining at $-30\text{ }^\circ\text{C}$, leading to a total reaction volume of 600 μL . The tube was sealed immediately, quickly removed from the glovebox, and placed into an ethyl acetate/liquid nitrogen bath. It was well shaken to mix up all the components and immediately placed in the NMR probe that was pre-adjusted to 298.1 K. The product concentration was monitored at 60 s intervals for 2 h to determine the initial reaction rate.

9.1 Pre-catalyst **1** rate order assessment based on initial-rate kinetics

Varying concentrations of **1** while keeping constant concentrations of HBpin and isoquinoline.

$c_{cat \text{ 1}}$ (M)	c_{HBpin} (M)	$c_{isoquinoline}$ (M)	v_i (M/s)	R^2
0.0060	0.34	0.34	$8.60 \times 10^{-5} \pm 1.49 \times 10^{-6}$	0.99492
0.0050	0.34	0.34	$6.88 \times 10^{-5} \pm 1.60 \times 10^{-6}$	0.99828
0.0040	0.34	0.34	$5.57 \times 10^{-5} \pm 1.29 \times 10^{-7}$	0.98935
0.0030	0.34	0.34	$4.08 \times 10^{-5} \pm 1.05 \times 10^{-7}$	0.98701
0.0020	0.34	0.34	$2.87 \times 10^{-5} \pm 5.61 \times 10^{-7}$	0.99243
0.0015	0.34	0.34	$2.08 \times 10^{-5} \pm 4.90 \times 10^{-7}$	0.98905

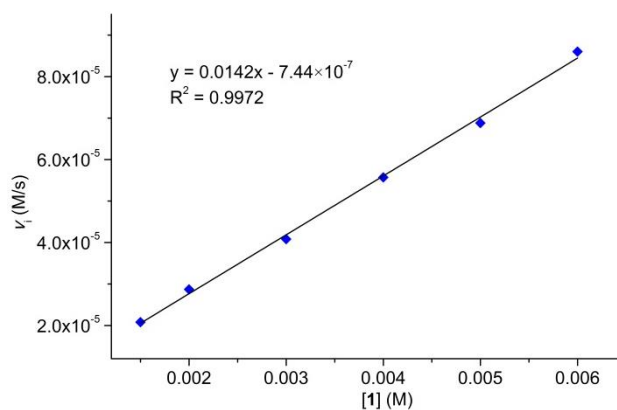


Figure S13. Plot of $[1]$ vs. reaction rate, the reaction follows first order dependence on **1** over the probed concentration range.

9.2 Isoquinoline rate order assessment

Varying concentrations of isoquinoline while keeping constant concentrations of HBpin and

1.

$c_{\text{isoquinoline}}$ (M)	c_{HBpin} (M)	c_1 (M)	v_i (M/s)	R^2
0.20	0.20	0.0020	$2.47 \times 10^{-5} \pm 4.68 \times 10^{-7}$	0.99322
0.30	0.20	0.0020	$2.47 \times 10^{-5} \pm 3.96 \times 10^{-7}$	0.99488
0.50	0.20	0.0020	$2.54 \times 10^{-5} \pm 4.27 \times 10^{-7}$	0.99493
0.60	0.20	0.0020	$2.38 \times 10^{-5} \pm 4.95 \times 10^{-7}$	0.99185

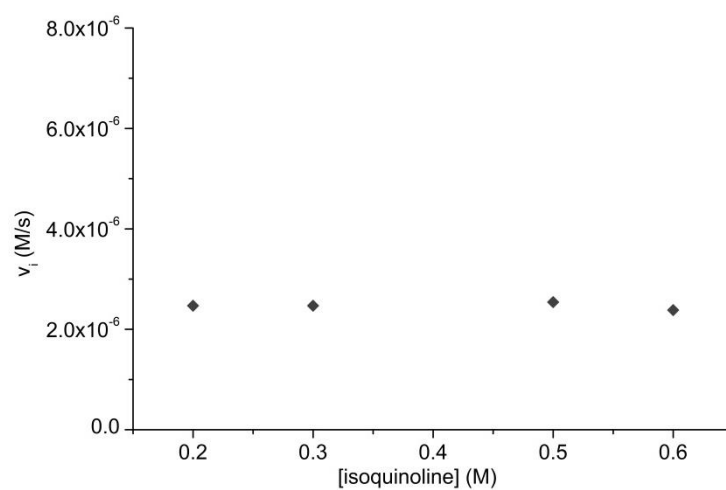


Figure S14. Plot of [isoquinoline] vs. reaction rate, the reaction follows zero order dependence on isoquinoline over the probed concentration range.

9.3 HBpin rate order assessment

Varying concentrations of HBpin while keeping constant concentrations of isoquinoline and

1.

c_{HBpin} (M)	$c_{\text{isoquinoline}}$ (M)	c_1 (M)	v_i (M/s)	R^2
0.20	0.33	0.0033	$3.27 \times 10^{-5} \pm 6.29 \times 10^{-7}$	0.99266
0.33	0.33	0.0033	$5.67 \times 10^{-5} \pm 7.59 \times 10^{-7}$	0.99643
0.40	0.33	0.0033	$6.84 \times 10^{-5} \pm 1.29 \times 10^{-6}$	0.99613
0.67	0.33	0.0033	$1.09 \times 10^{-4} \pm 1.66 \times 10^{-6}$	0.99769
0.93	0.33	0.0033	$1.55 \times 10^{-4} \pm 2.09 \times 10^{-6}$	0.99820

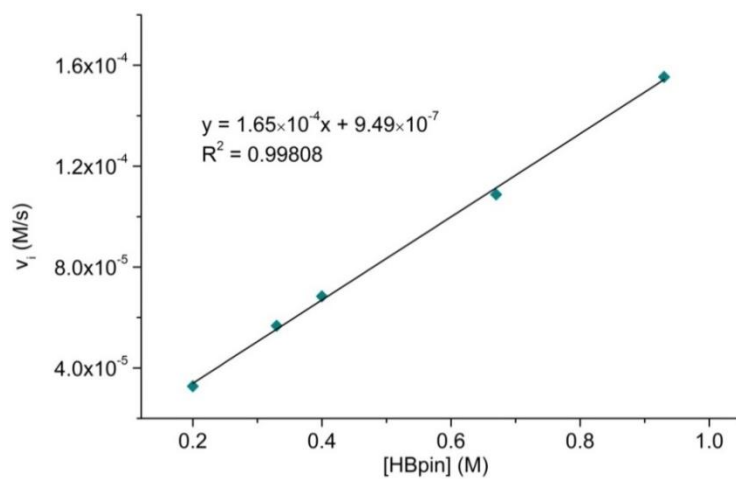
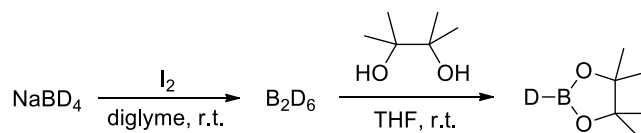


Figure S15. Plot of [HBpin] vs. reaction rate, the reaction follows first order dependence on HBpin over the probed concentration range.

9.4 Determination of the kinetic isotope effect

Preparation of DBpin

*d*₁-pinacolborane was prepared according to the reported procedures.¹⁰



¹H NMR (500 MHz, C₆D₆): δ 0.99 (s, 12H).

²H NMR (77 MHz, benzene): δ 4.23 (br, d).

¹¹B NMR (160 MHz, C₆D₆): δ 28.49 (s).

Determination of the kinetic isotope effect

KIE was determined using standard condition, data points were collected at 60 s intervals over 2 h at 298.1 K, data points before 23% conversion were subjected to the liner regression analysis.

1	isoquinoline	HBpin (1.2 eq)	tetraethylsilane
0.0020 mmol	0.20 mmol	0.24 mmol	0.025 mmol
0.0033 M	0.33 M	0.40 M	0.042 M

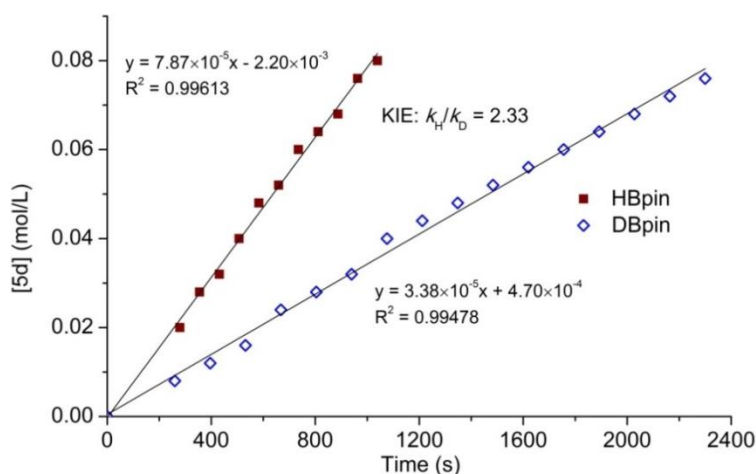
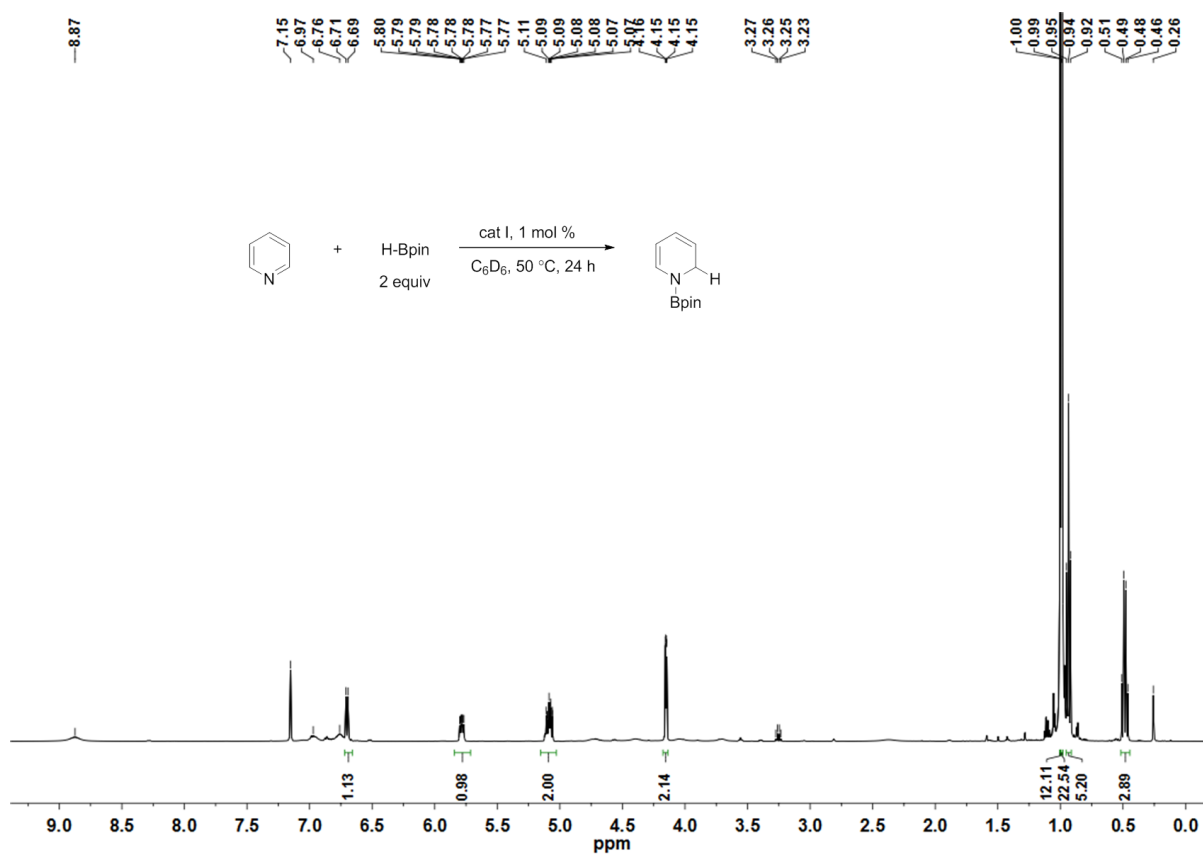
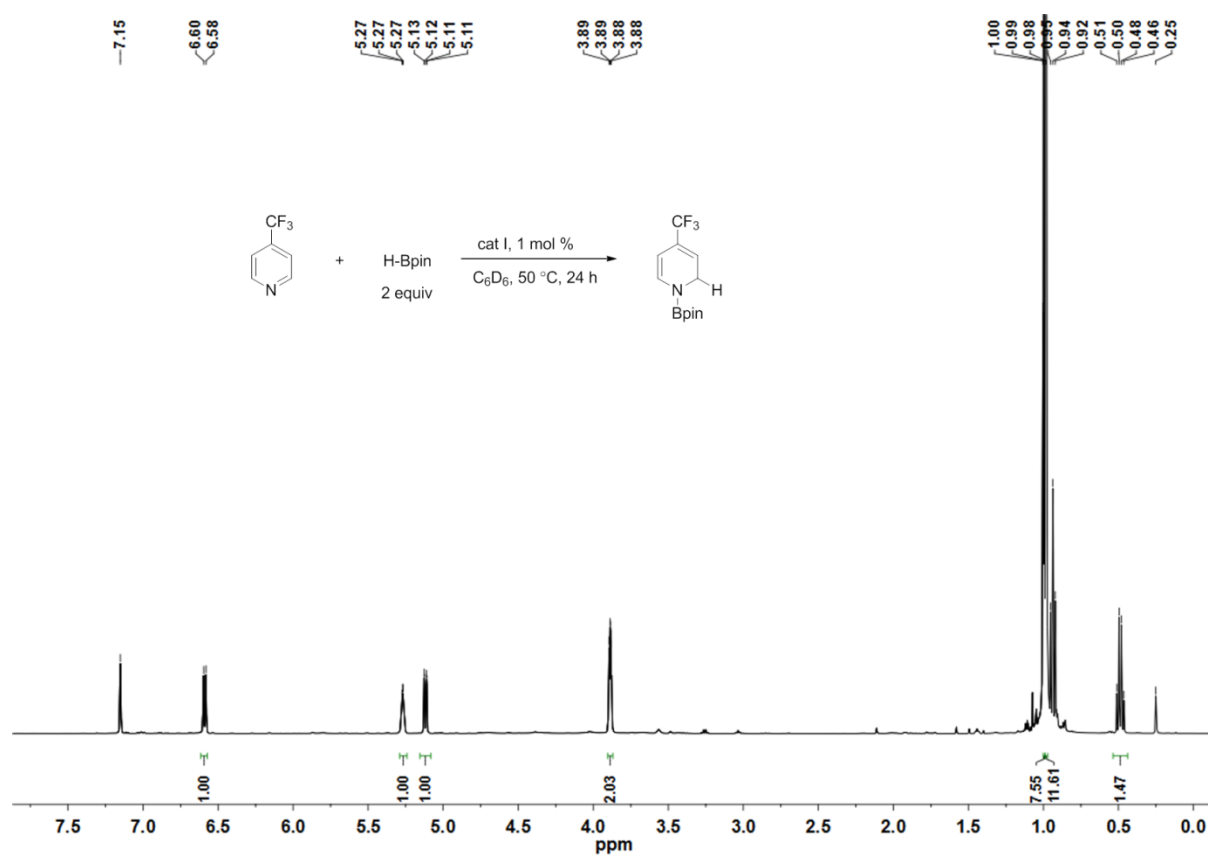


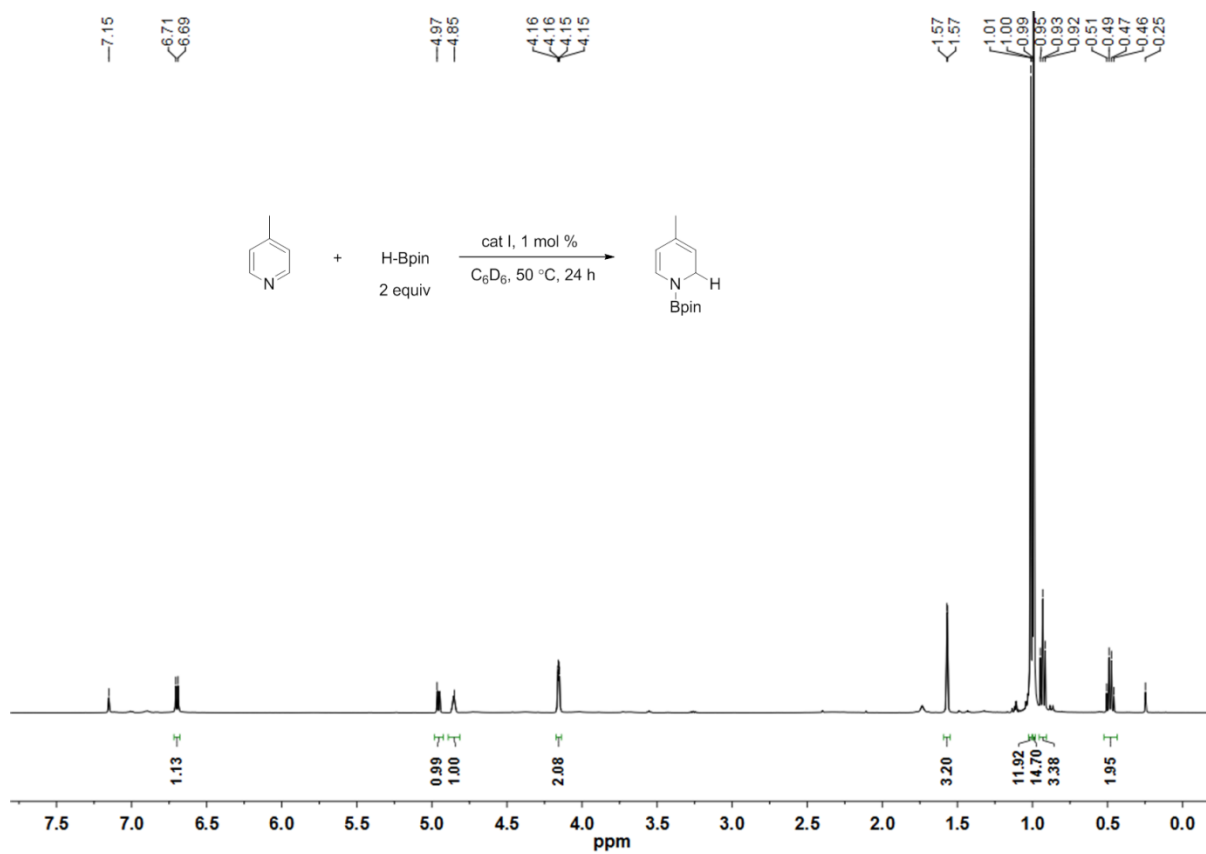
Figure S16. KIE for hydroboration of isoquinoline.

10. ^1H NMR and ^{13}C spectra

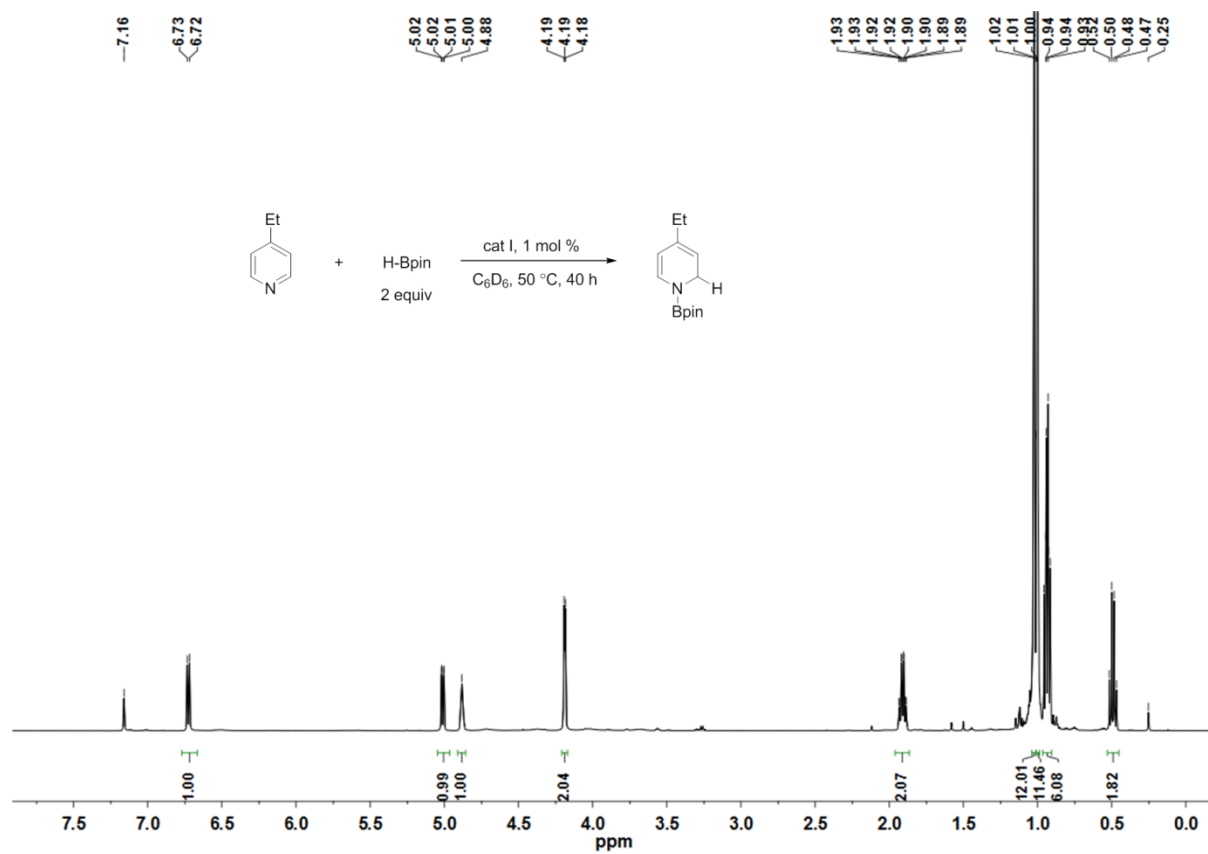
Assignment: pyridine, δ 8.87, 6.97, 6.76; diethyl ether, δ 3.25, 1.11; tetraethylsilane (I.S.), δ 0.94, 0.49; silicone grease, δ 0.26.



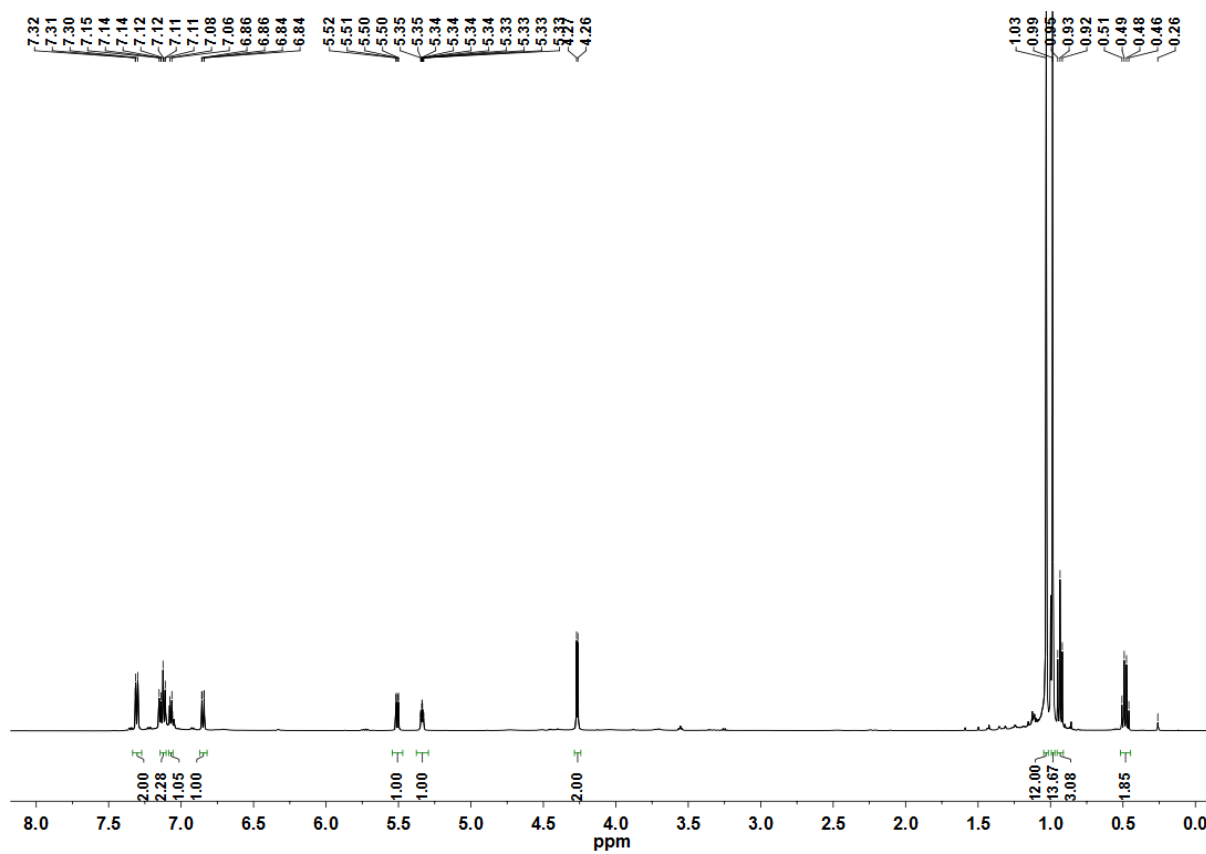
Assignment: diethyl ether, δ 3.25, 1.11; tetraethylsilane (I.S.), δ 0.94, 0.50; silicone grease, δ 0.25.



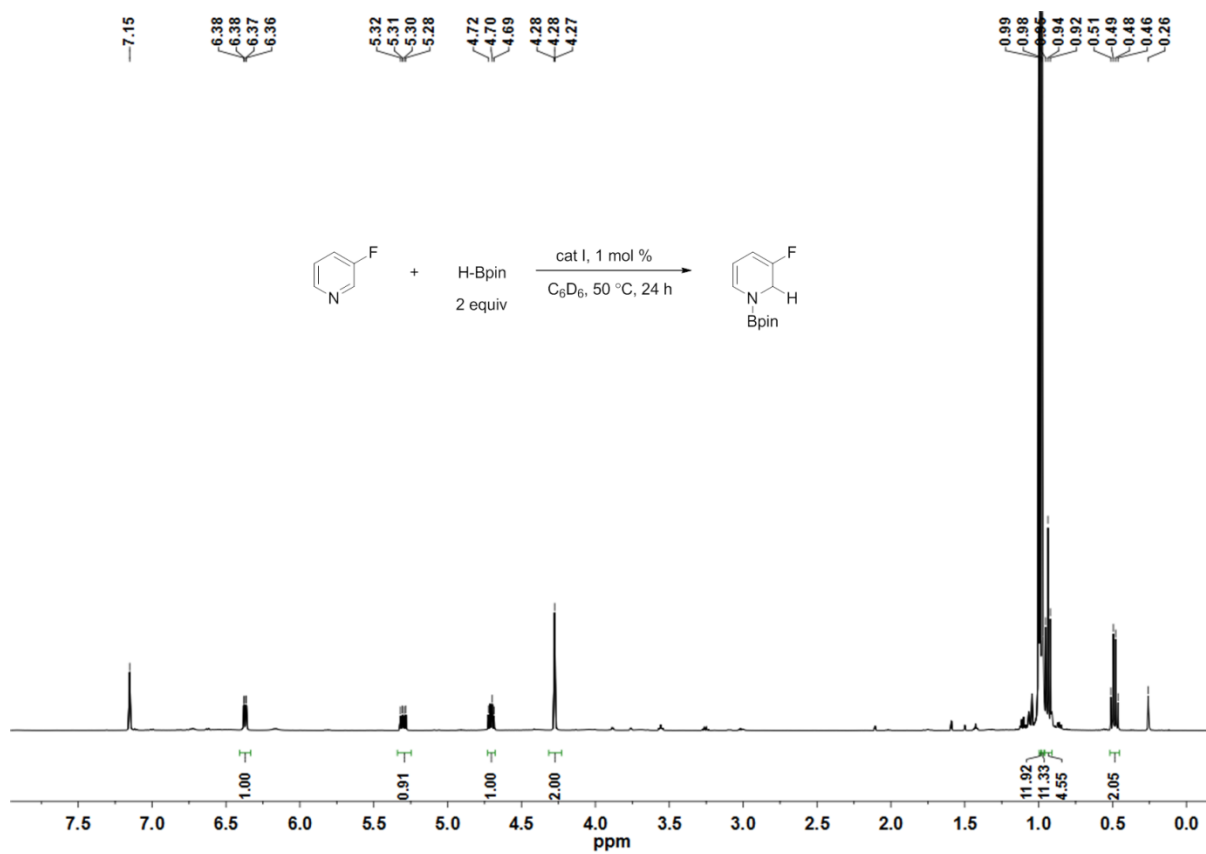
Assignment: 4-methylpyridine, δ 1.73; diethyl ether, δ 3.25, 1.11; tetraethylsilane (I.S.), δ 0.93, 0.49; silicone grease, δ 0.25.



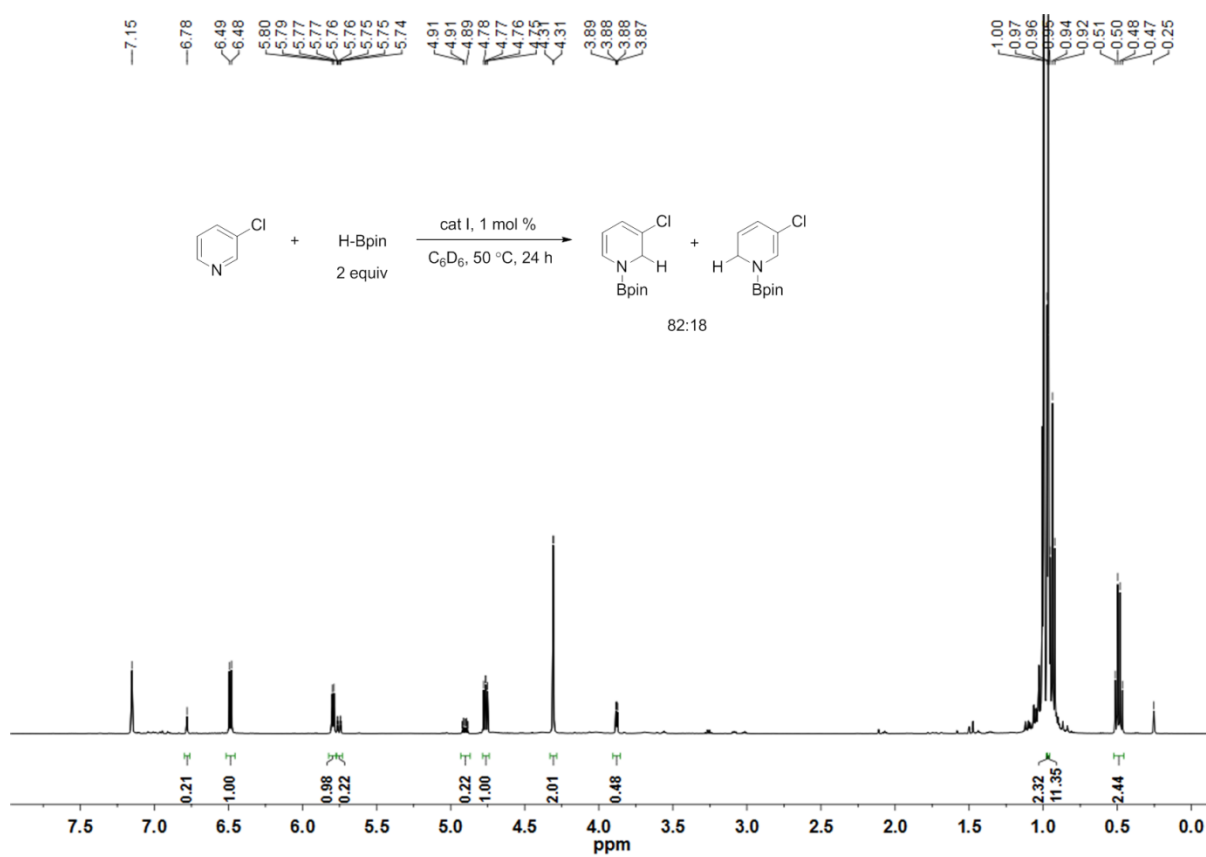
Assignment: diethyl ether, δ 3.25, 1.11; tetraethylsilane (I.S.), δ 0.94, 0.50; silicone grease, δ 0.25.



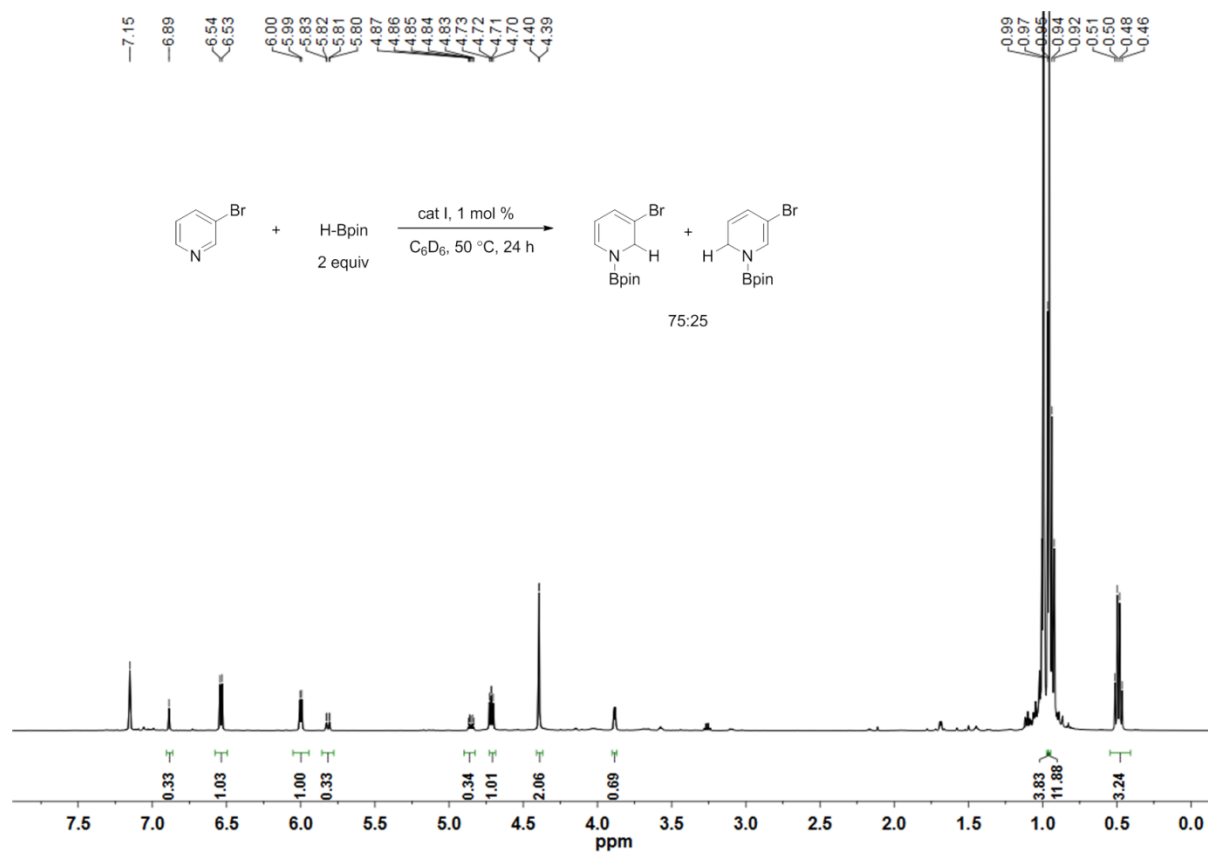
Assignment: diethyl ether, δ 3.25, 1.11; tetraethylsilane (I.S.), δ 0.93, 0.49; silicone grease, δ 0.25.



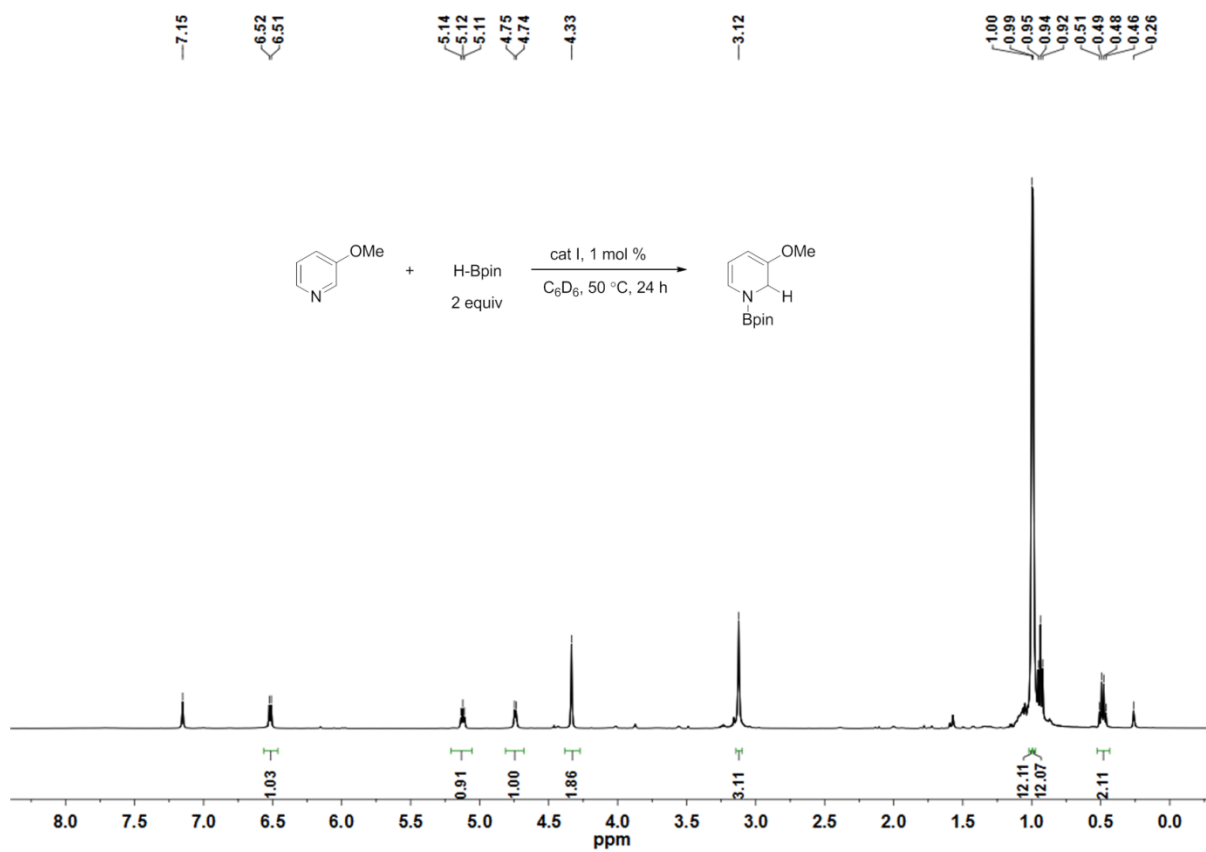
Assignment: THF, δ 3.57, 1.40; diethyl ether, δ 3.25, 1.11; tetraethylsilane (I.S.), δ 0.94, 0.49; silicone grease, δ 0.26.



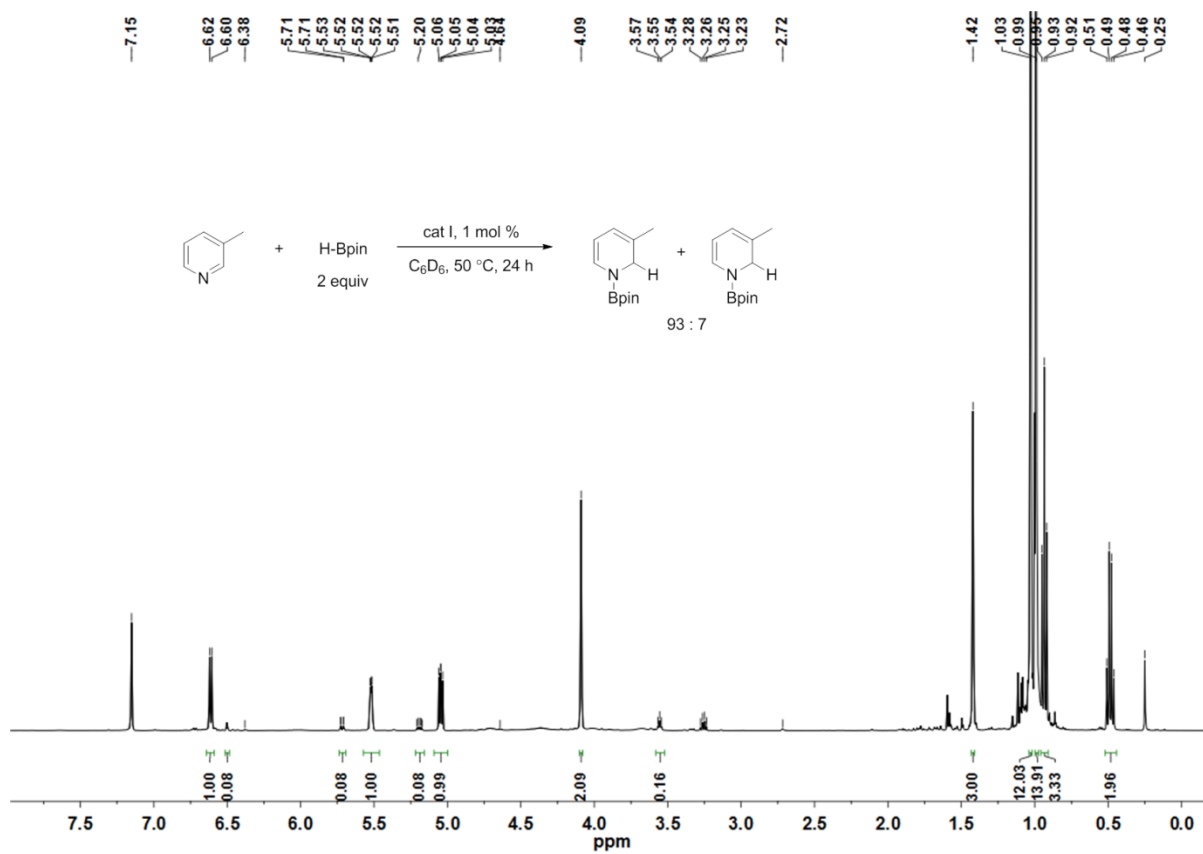
Assignment: diethyl ether, δ 3.25, 1.11; tetraethylsilane (I.S.), δ 0.94, 0.50; silicone grease, δ 0.25.



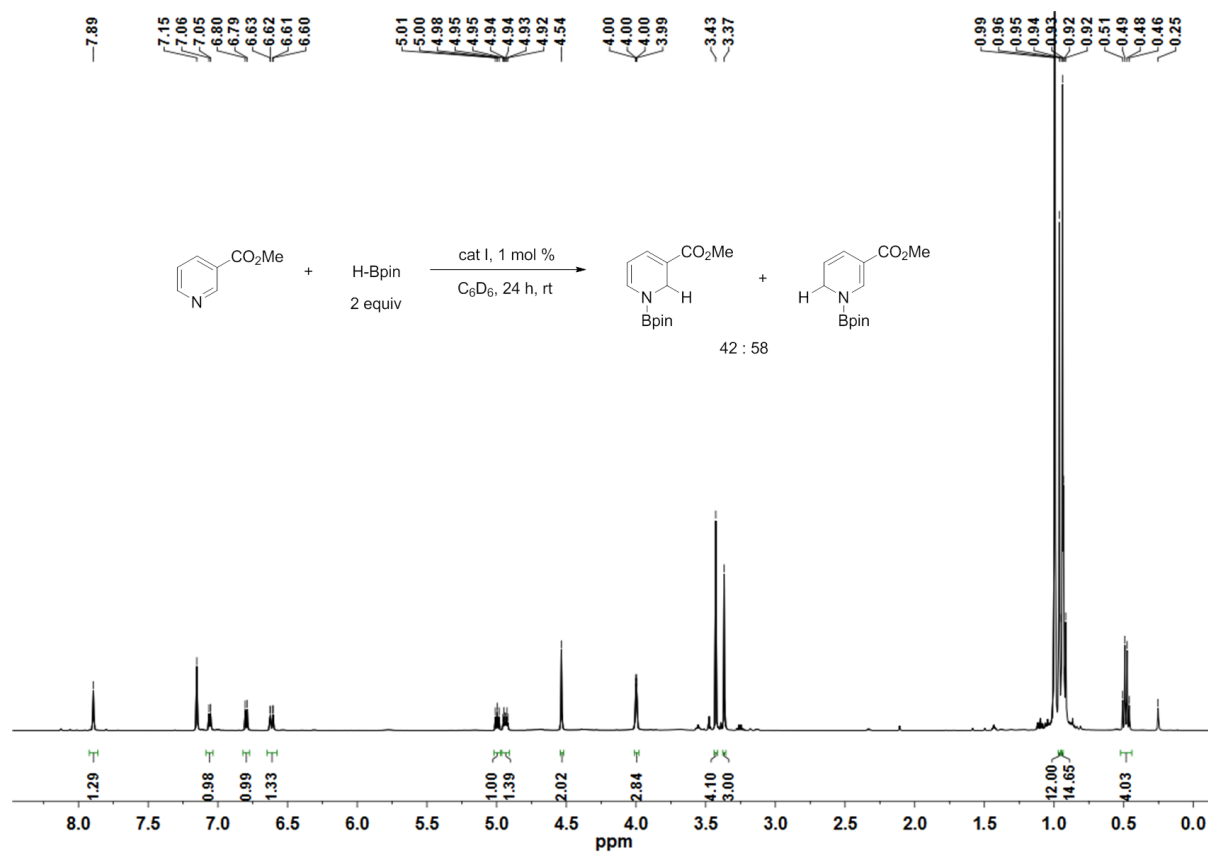
Assignment: THF, δ 3.57, 1.40; diethyl ether, δ 3.25, 1.11; tetraethylsilane (I.S.), δ 0.94, 0.50.



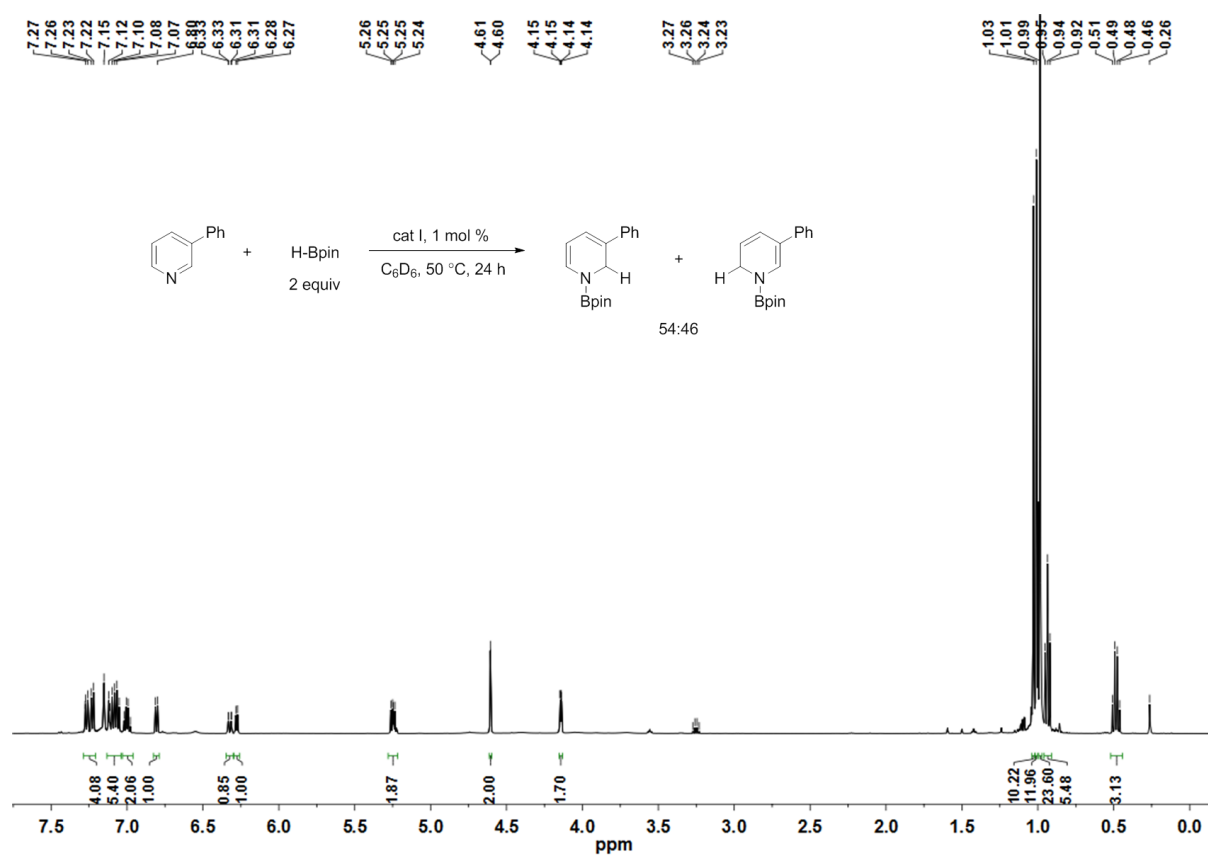
Assignment: tetraethylsilane (I.S.), δ 0.94, 0.49; silicone grease, δ 0.26.



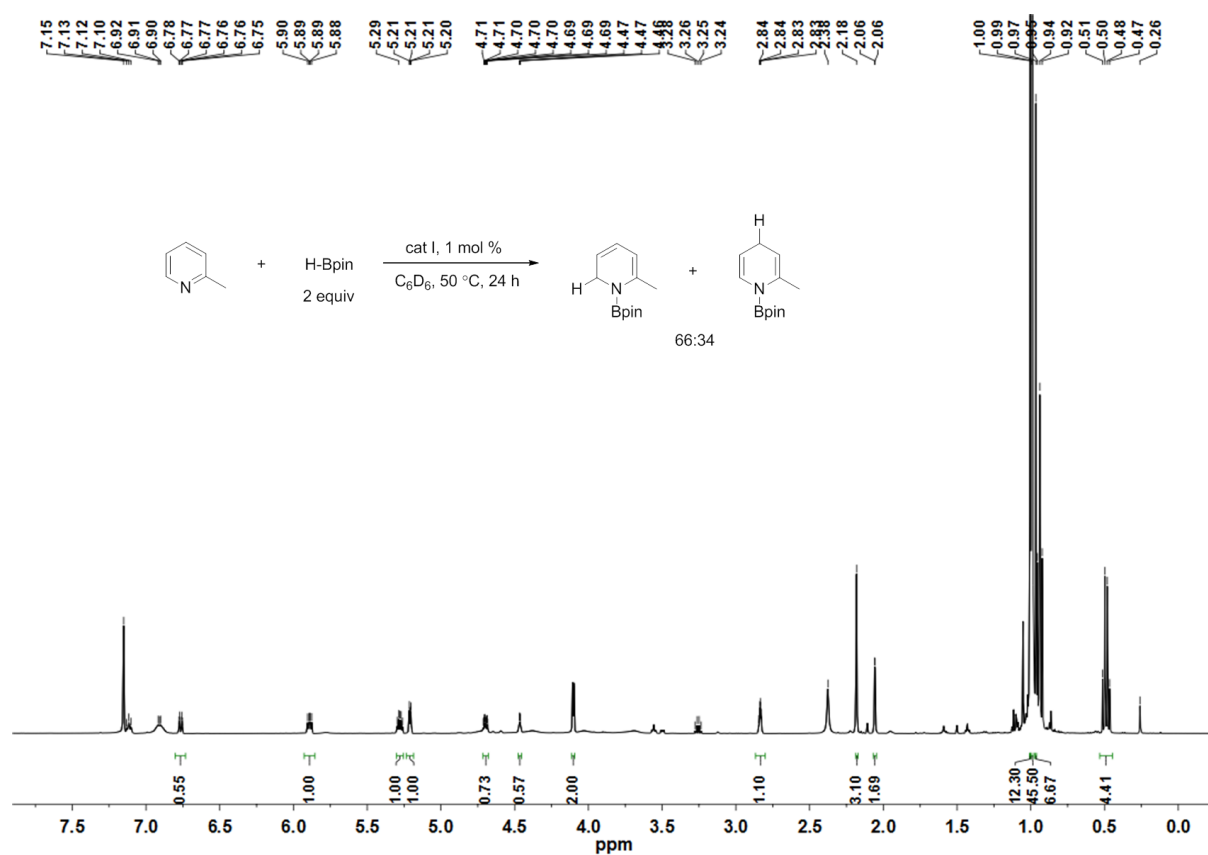
Assignment: diethyl ether, δ 3.25, 1.11; tetraethylsilane (I.S.), δ 0.93, 0.49; silicone grease, δ 0.25.



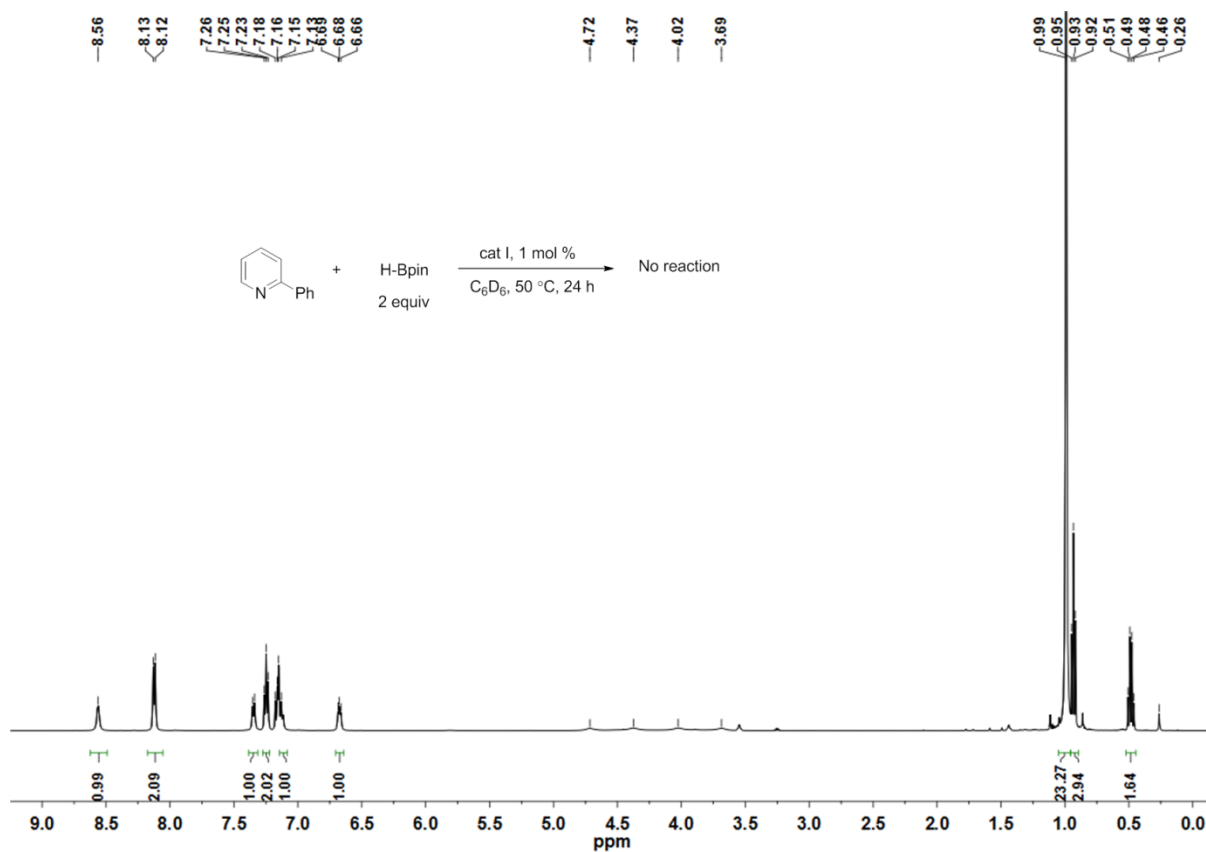
Assignment: THF, δ 3.57, 1.40; diethyl ether, δ 3.25, 1.11; tetraethylsilane (I.S.), δ 0.92, 0.49; silicone grease, δ 0.25.



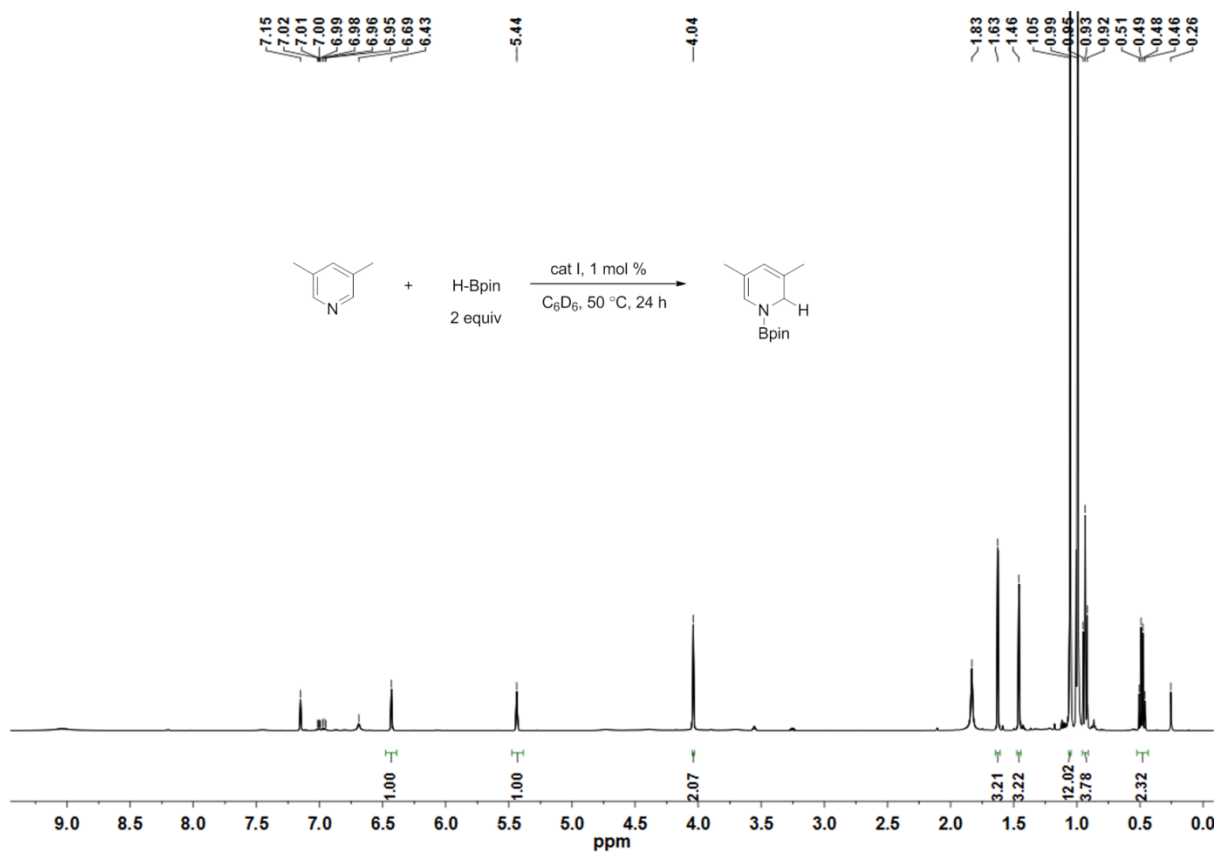
Assignment: THF, δ 3.57, 1.40; diethyl ether, δ 3.26, 1.11; tetraethylsilane (I.S.), δ 0.94, 0.49; silicone grease, δ 0.26.



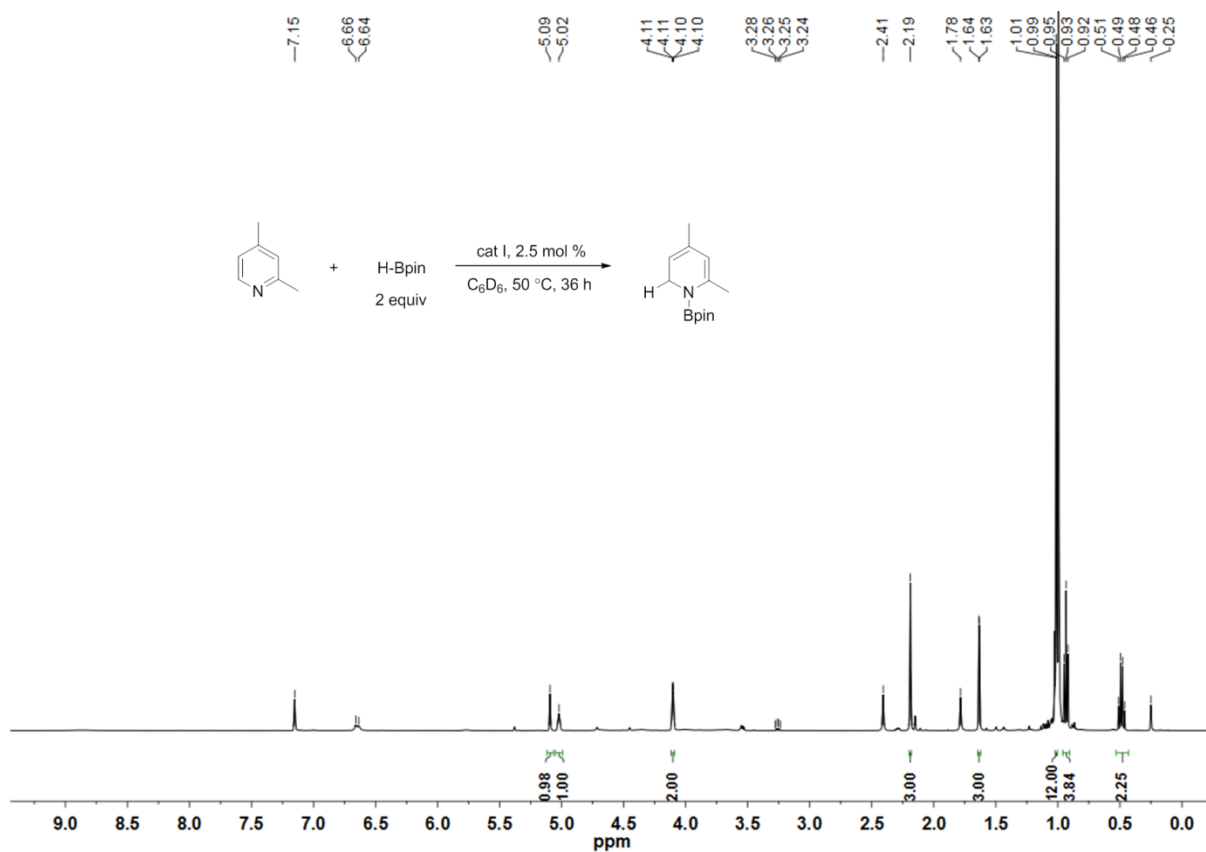
Assignment: 2-methylpyridine, δ 7.12, 6.91, 2.38; THF, δ 3.57, 1.40; diethyl ether, δ 3.26, 1.11; tetraethylsilane (I.S.), δ 0.94, 0.50; silicone grease, δ 0.26.



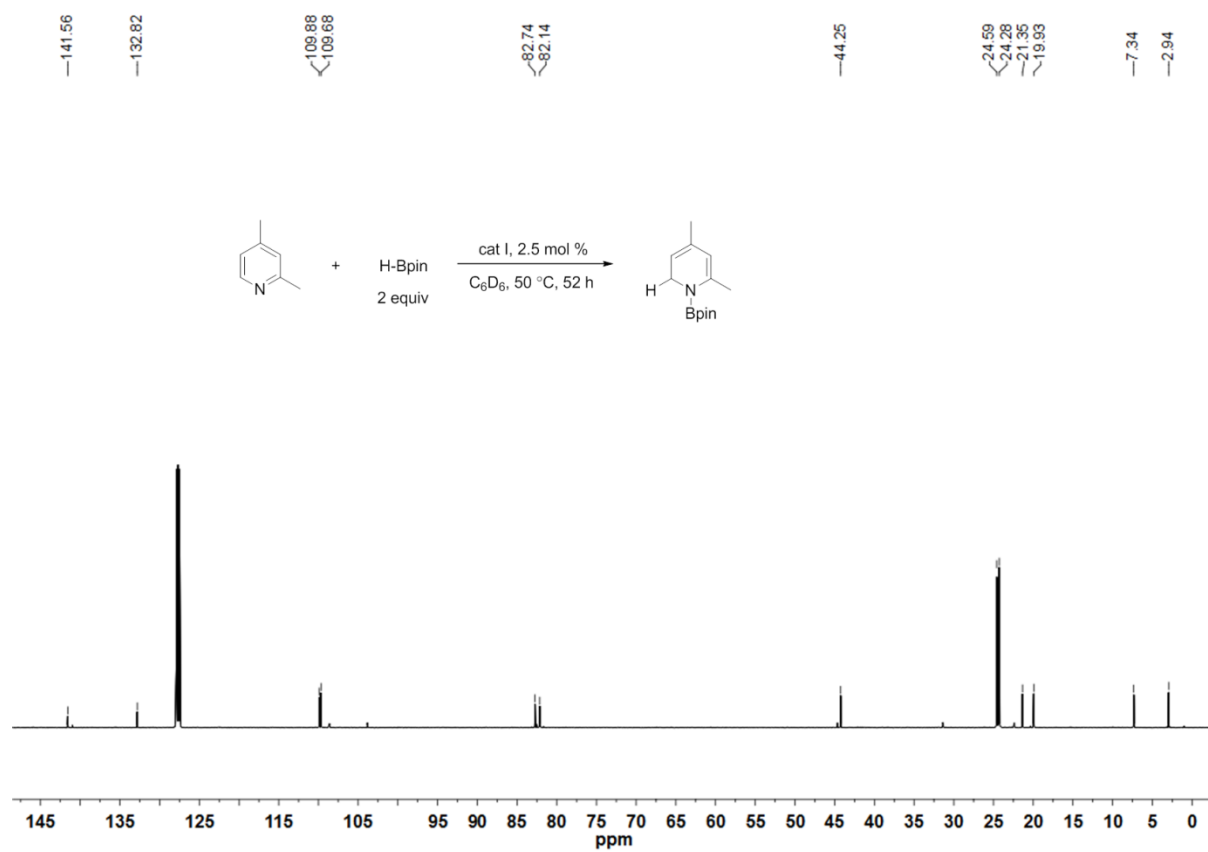
Assignment: THF, δ 3.57, 1.40; diethyl ether, δ 3.26, 1.11; tetraethylsilane (I.S.), δ 0.93, 0.49; silicone grease, δ 0.26.



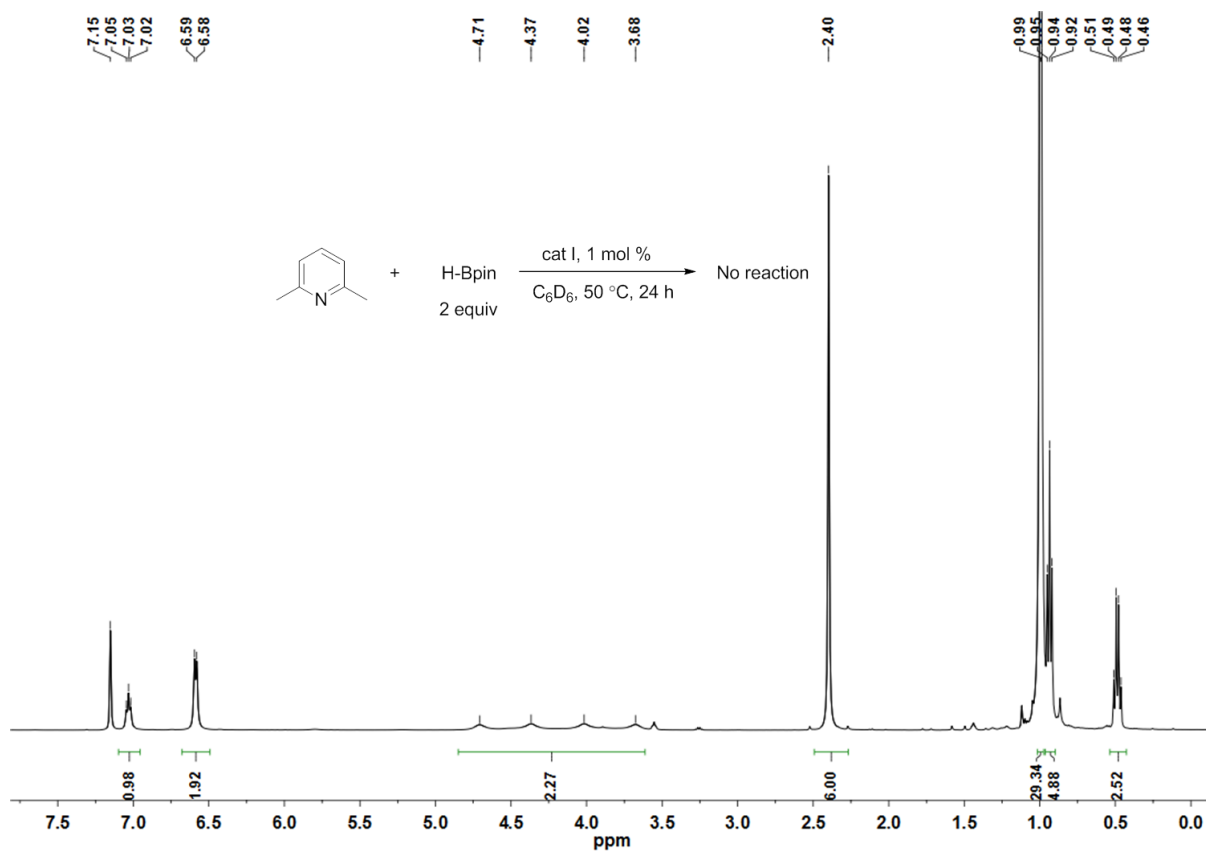
Assignment: 3,5-dimethylpyridine, δ 6.96, 6.69, 1.83; THF, δ 3.57, 1.40; diethyl ether, δ 3.26, 1.11; tetraethylsilane (I.S.), δ 0.93, 0.49; silicone grease, δ 0.26.



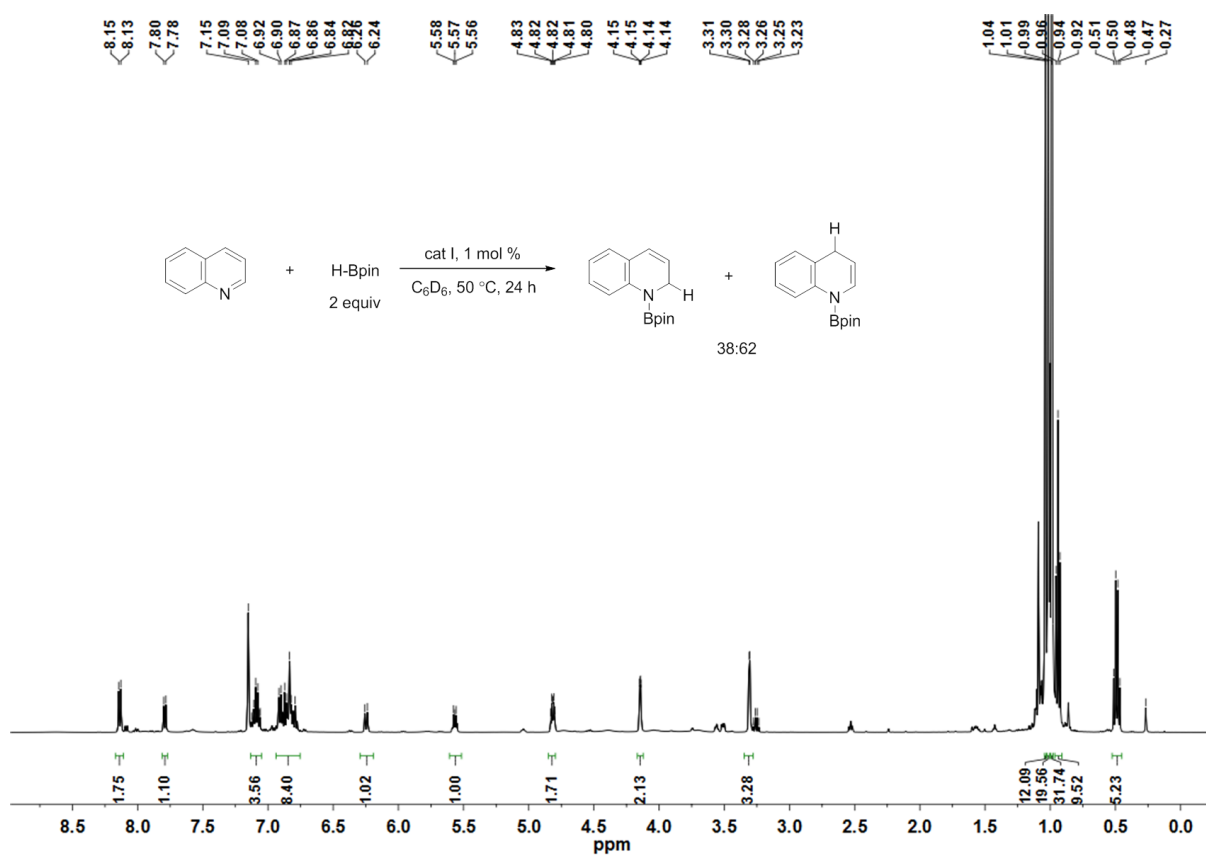
Assignment: 2,4-dimethylpyridine, δ 6.66, 2.41, 1.78; THF, δ 3.57, 1.40; diethyl ether, δ 3.26, 1.11; tetraethylsilane (I.S.), δ 0.93, 0.49; silicone grease, δ 0.25.



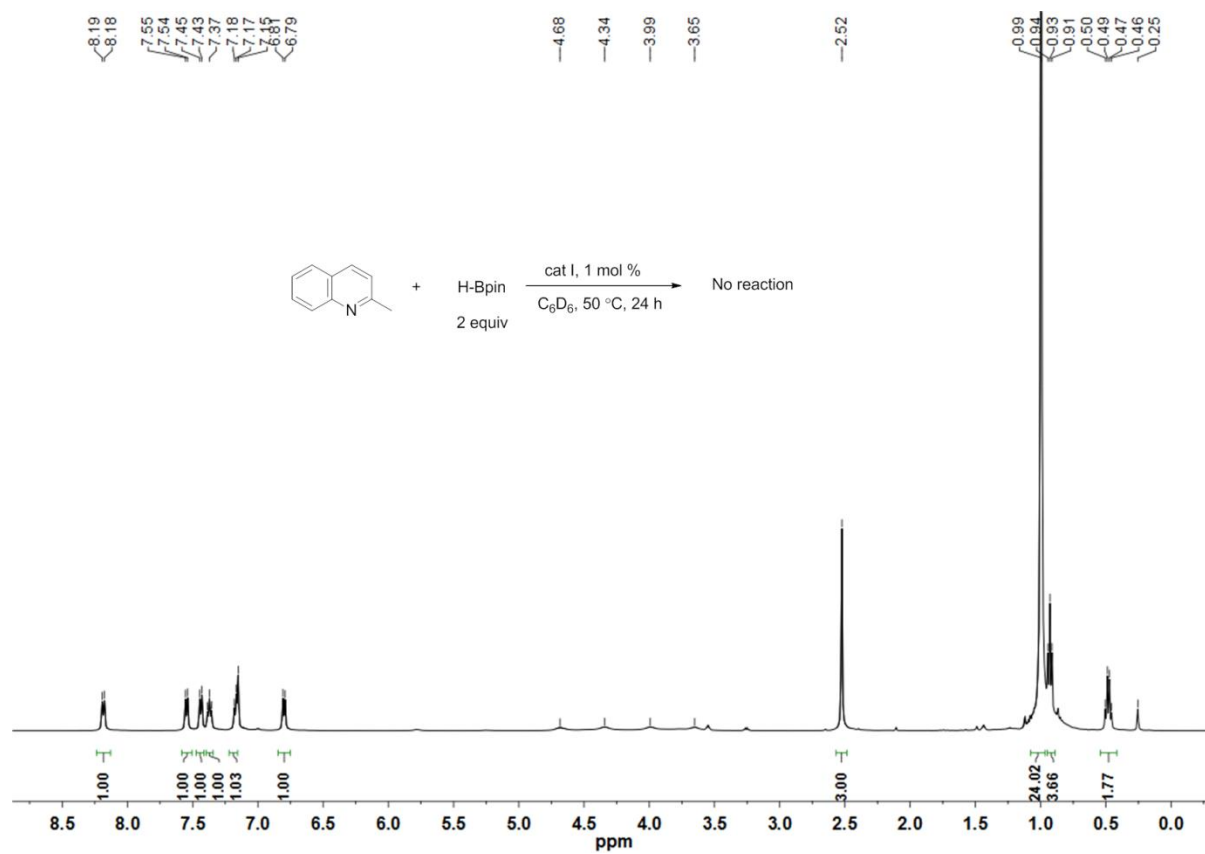
Assignment: HBpin, δ 82.74, 24.59; tetraethylsilane (I.S.), δ 7.34, 2.94.



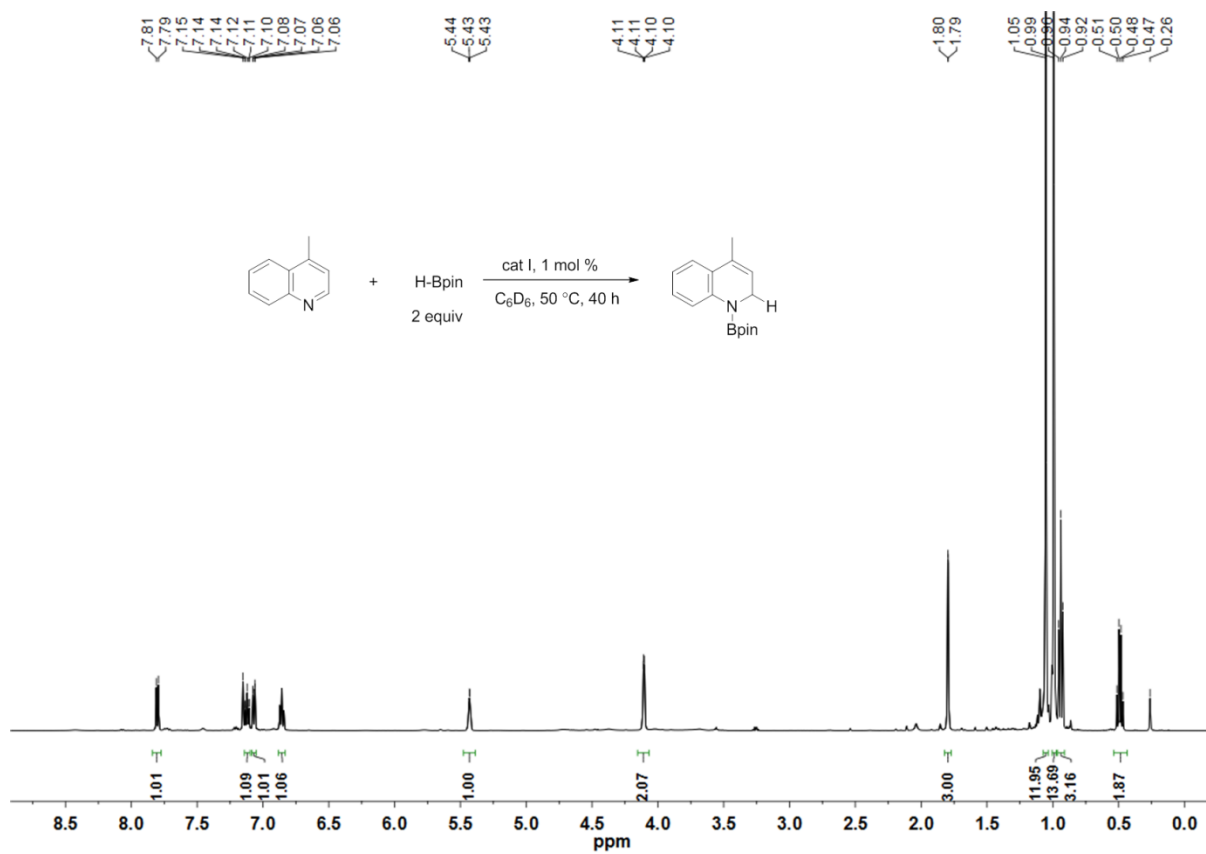
Assignment: THF, δ 3.57, 1.40; diethyl ether, δ 3.26, 1.11; tetraethylsilane (I.S.), δ 0.94, 0.49.



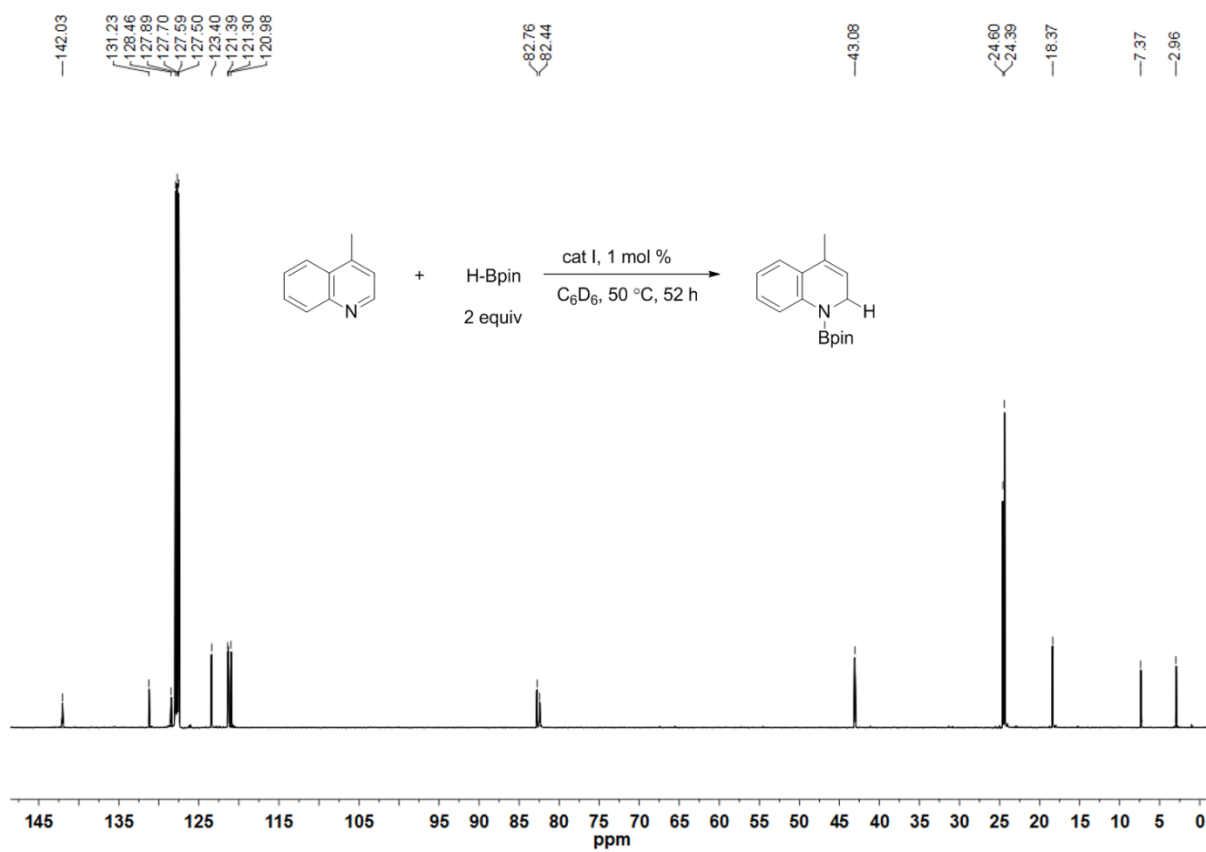
Assignment: THF, δ 3.57, 1.40; diethyl ether, δ 3.25, 1.11; tetraethylsilane (I.S.), δ 0.94, 0.50; silicone grease, δ 0.27.



Assignment: THF, δ 3.57, 1.40; tetraethylsilane (I.S.), δ 0.93, 0.49; silicone grease, δ 0.25.

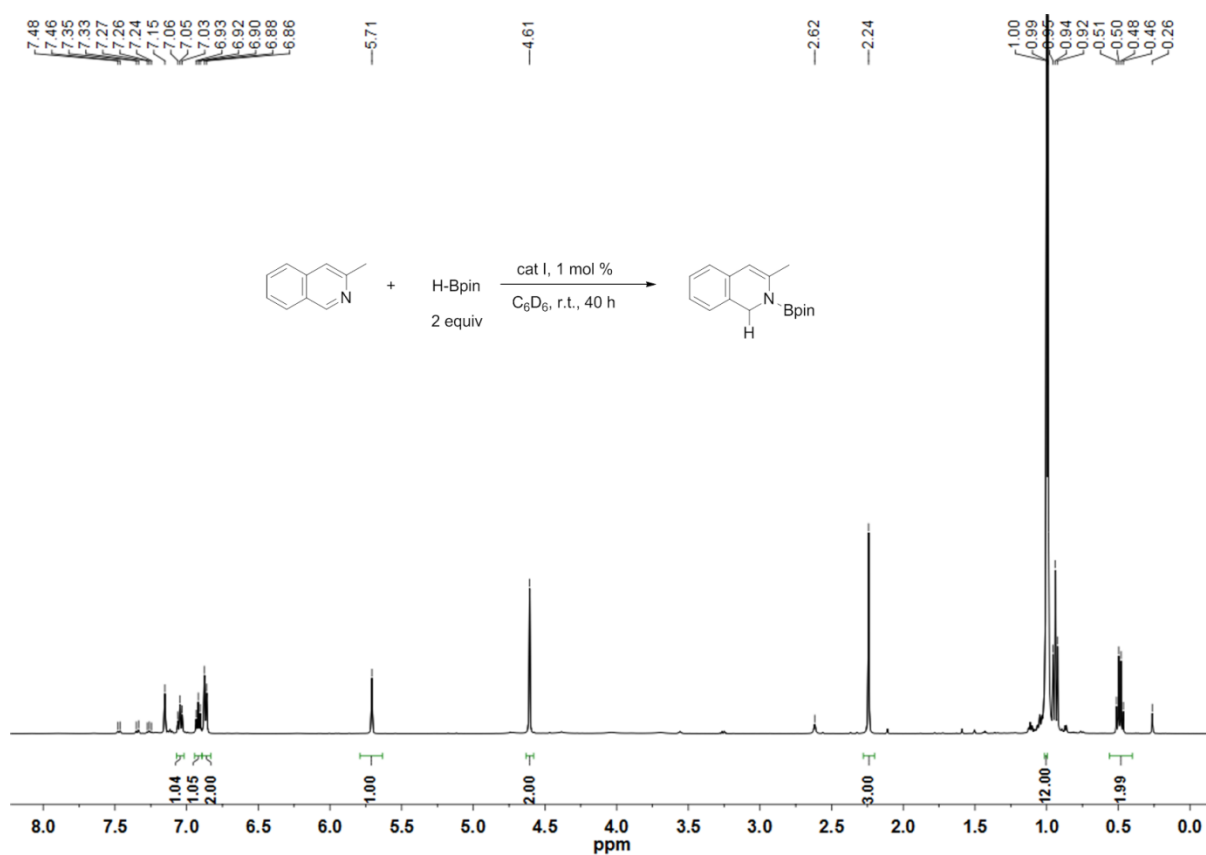


Assignment: diethyl ether, δ 3.25, 1.11; tetraethylsilane (I.S.), δ 0.94, 0.50; silicone grease, δ 0.26.

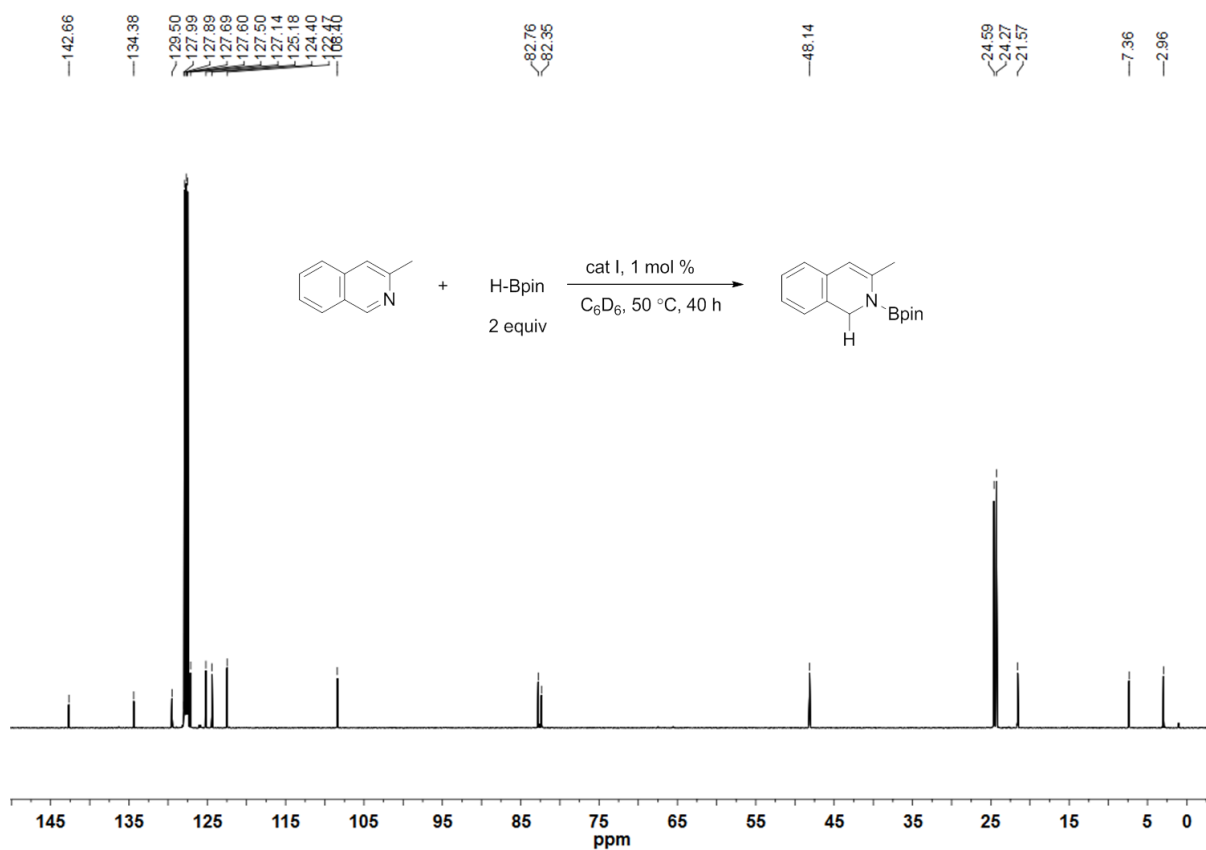


Assignment: HBpin, δ 82.76, 24.59; tetraethylsilane (I.S.), δ 7.37, 2.96.

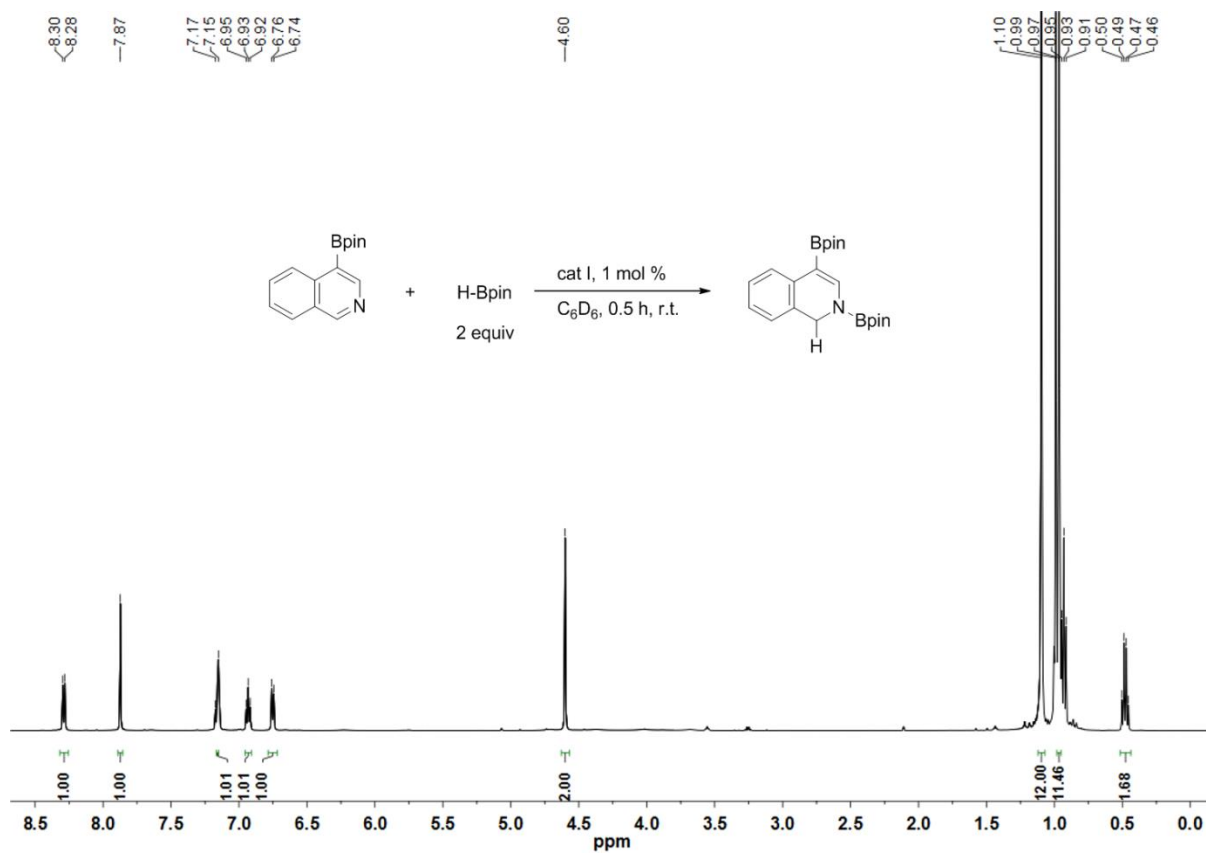
Assignment: diethyl ether, δ 3.25, 1.11; tetraethylsilane (I.S.), δ 0.94, 0.50.



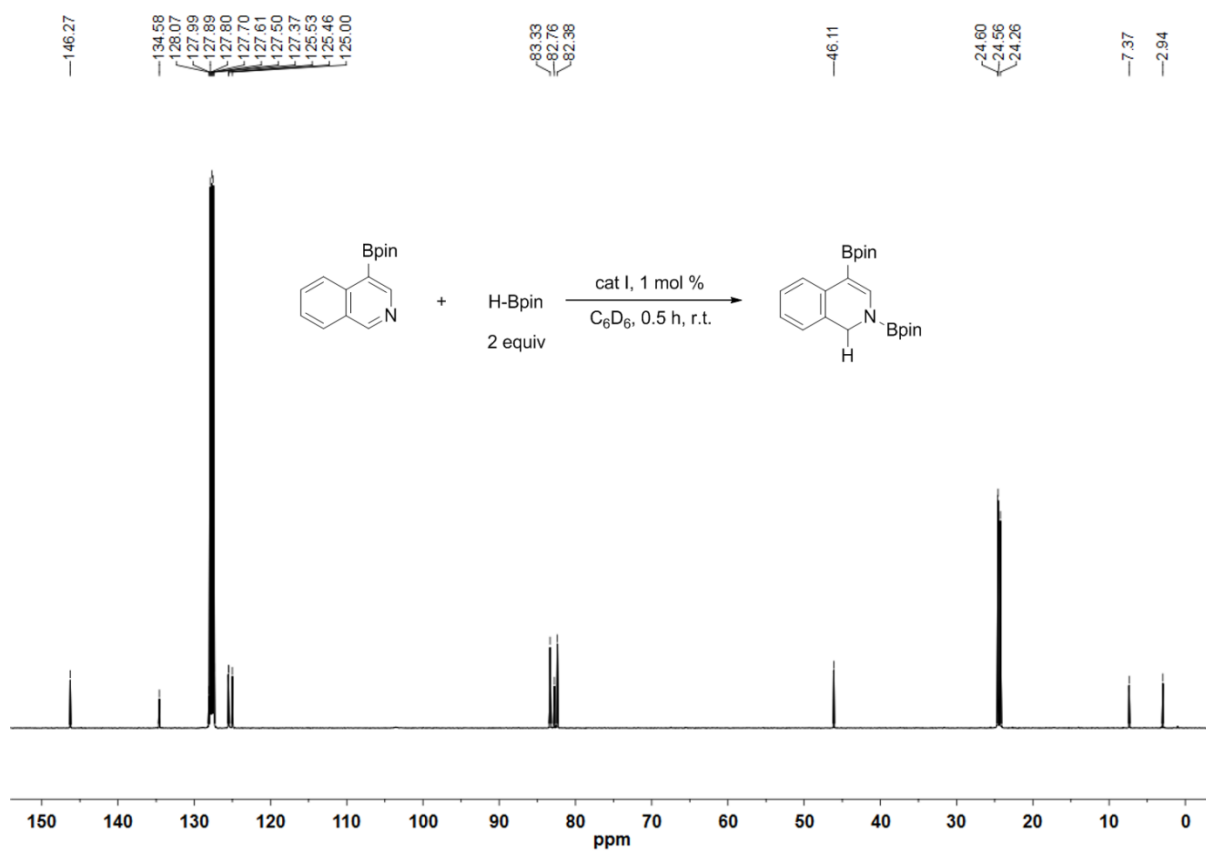
Assignment: 3-methylisoquinoline, δ 7.46, 7.33, 7.26, 2.62; diethyl ether, δ 3.25, 1.11; tetraethylsilane (I.S.), δ 0.94, 0.50; silicone grease, δ 0.26.



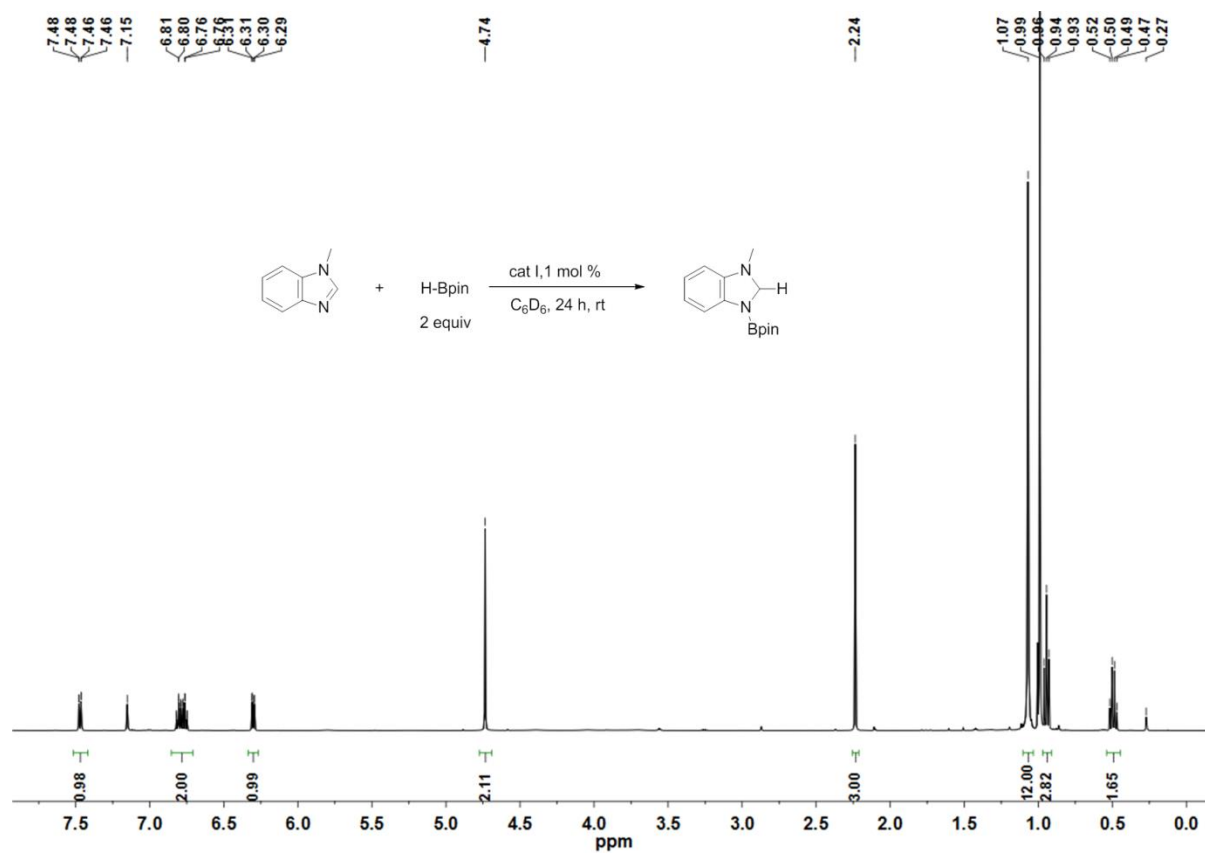
Assignment: HBpin, δ 82.76, 24.59; tetraethylsilane (I.S.), δ 7.36, 2.96.



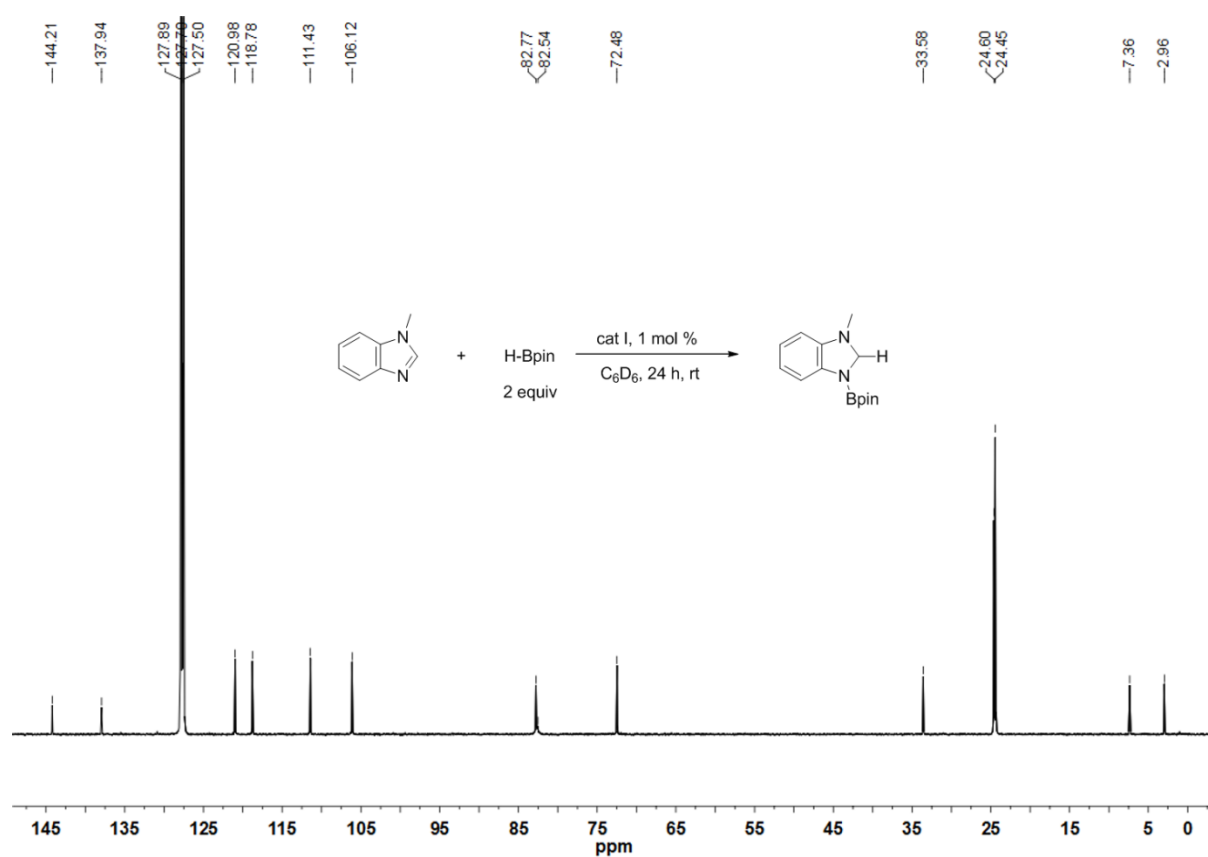
Assignment: THF, δ 3.57, 1.40; diethyl ether, δ 3.25, 1.11; tetraethylsilane (I.S.), δ 0.93, 0.49.



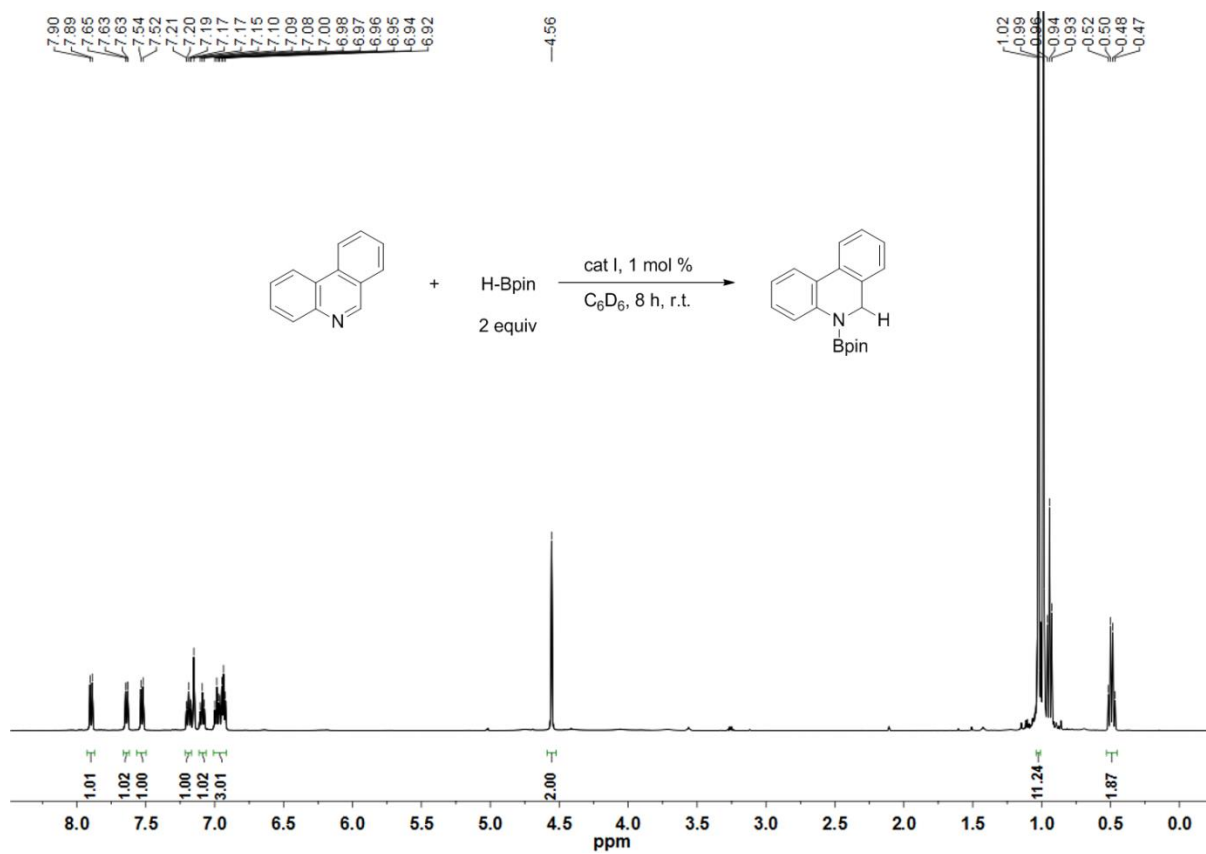
Assignment: HBpin, δ 82.76, 24.60; tetraethylsilane (I.S.), δ 7.37, 2.94.



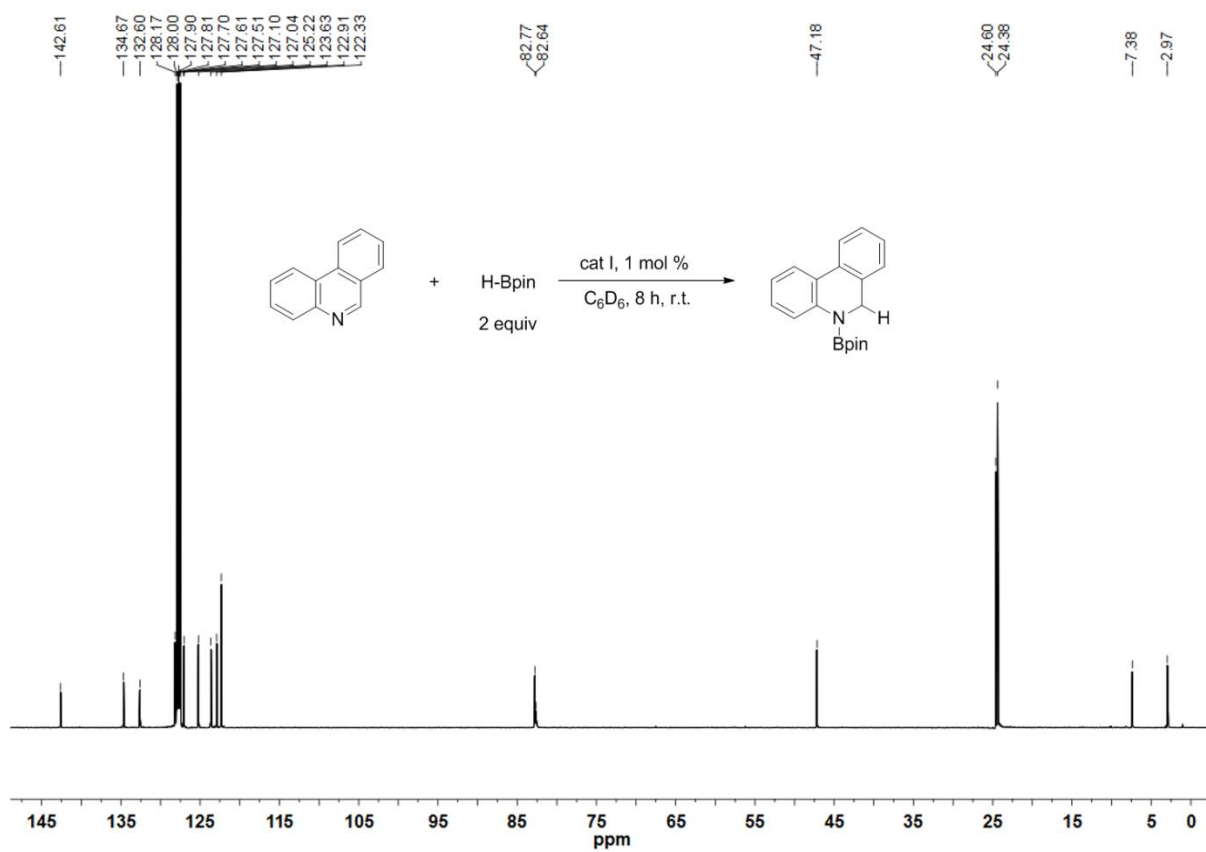
Assignment: THF, δ 3.57, 1.40; tetraethylsilane (I.S.), δ 0.94, 0.50; silicone grease, δ 0.27.



Assignment: HBpin, δ 82.77, 24.60; tetraethylsilane (I.S.), δ 7.36, 2.96.



Assignment: THF, δ 3.57, 1.40; diethyl ether, δ 3.25, 1.11; tetraethylsilane (I.S.), δ 0.94, 0.50.



Assignment: HBpin, δ 82.77, 24.60; tetraethylsilane (I.S.), δ 7.38, 2.97.

11. X-ray crystal structure analysis

Table S5. Crystal data and structure refinement of complexes **1**, **5 h**, **6** and **7**.

	1	5h	6	7
Empirical formula	C ₅₆ H ₅₈ Fe ₂ N ₂ P ₂ S ₂	C ₃₈ H ₄₄ B ₂ N ₂ O ₄	C ₃₇ H ₃₆ FeNPS	C ₃₃ H ₃₄ FeNPS
Formula weight	996.80	614.37	613.55	563.49
Temperature / K	173	100.01(10)	192.99(10)	173(2)
Crystal system	monoclinic	monoclinic	monoclinic	monoclinic
Space group	P2 ₁ /c	P2/c	P2 ₁ /c	Cc
<i>a</i> / Å	11.3448(9)	14.8368(3)	20.803(4)	19.063(6)
<i>b</i> / Å	18.9750(14)	12.6939(2)	9.7913(11)	9.464(3)
<i>c</i> / Å	12.4207(9)	17.8201(3)	15.7087(17)	16.113(5)
<i>α</i> / °	90	90	90	90
<i>β</i> / °	117.621(5)	94.8640(18)	106.209(16)	103.953(3)
<i>γ</i> / °	90	90	90	90
Volume / Å ³	2369.1(3)	3344.10(11)	3072.5(8)	2821.1(15)
Z	2	4	4	4
ρ_{calc} / g cm ⁻³	1.397	1.220	1.326	1.327
μ / mm ⁻¹	0.809	0.609	5.256	0.688
F(000)	1044.0	1312	1288.0	1184.0
2 θ range for data collection / °	5.664 to 55.004	5.978 to 142.12	8.854 to 134.102	4.398 to 49.994
Index ranges	-7 ≤ <i>h</i> ≤ 14, -24 ≤ <i>k</i> ≤ 15, -16 ≤ <i>l</i> ≤ 9	-11 ≤ <i>h</i> ≤ 17, -15 ≤ <i>k</i> ≤ 11, -21 ≤ <i>l</i> ≤ 21	-24 ≤ <i>h</i> ≤ 24, -4 ≤ <i>k</i> ≤ 11, -18 ≤ <i>l</i> ≤ 17	-22 ≤ <i>h</i> ≤ 22, -9 ≤ <i>k</i> ≤ 11, -18 ≤ <i>l</i> ≤ 19
Reflections collected	13399	12847	17209	8041
Independent reflections	5129 [<i>R</i> _{int} = 0.0598, <i>R</i> _{sigma} = 0.0943]	6345 [<i>R</i> _{int} = 0.0214, <i>R</i> _{sigma} = 0.0273]	5330 [<i>R</i> _{int} = 0.0971, <i>R</i> _{sigma} = 0.1050]	4179 [<i>R</i> _{int} = 0.0256, <i>R</i> _{sigma} = 0.0391]
Data/restraints/parameters	5129/0/294	6345/0/423	5330/0/375	4179/2/339
Goodness-of-fit on <i>F</i> ²	1.041	1.045	1.047	1.047
Final <i>R</i> indexes [<i>I</i> > 2σ(<i>I</i>)]	<i>R</i> ₁ = 0.0582 <i>wR</i> ₂ = 0.1121	<i>R</i> ₁ = 0.0446 <i>wR</i> ₂ = 0.1145	<i>R</i> ₁ = 0.0571 <i>wR</i> ₂ = 0.1176	<i>R</i> ₁ = 0.0238 <i>wR</i> ₂ = 0.0585
Final <i>R</i> indexes [all data]	<i>R</i> ₁ = 0.1198 <i>wR</i> ₂ = 0.1383	<i>R</i> ₁ = 0.0500 <i>wR</i> ₂ = 0.1192	<i>R</i> ₁ = 0.1142 <i>wR</i> ₂ = 0.1480	<i>R</i> ₁ = 0.0248 <i>wR</i> ₂ = 0.0592
Largest diff. peak/hole / e Å ⁻³	1.04/-0.84	0.30/-0.24	0.43/-0.52	0.24/-0.21

Table S6. Crystal data and structure refinement of complex **8**.

	8
Empirical formula	C ₃₄ H ₃₆ FeNPS
Formula weight	577.52
Temperature / K	172.99(10)
Crystal system	monoclinic
Space group	P2 ₁ /c
<i>a</i> / Å	18.5491(4)
<i>b</i> / Å	9.8654(3)
<i>c</i> / Å	15.8227(3)
α / °	90
β / °	91.771(2)
γ / °	90
Volume / Å ³	2894.08(12)
<i>Z</i>	4
ρ_{calc} / g cm ⁻³	1.325
μ / mm ⁻¹	0.672
F(000)	1216
2 Θ range for data collection / °	4.39 to 53.408
Index ranges	-22 ≤ <i>h</i> ≤ 23, -11 ≤ <i>k</i> ≤ 11, -19 ≤ <i>l</i> ≤ 16
Reflections collected	16605
Independent reflections	5660 [<i>R</i> _{int} = 0.0571, <i>R</i> _{sigma} = 0.0592]
Data/restraints/parameters	5660/0/349
Goodness-of-fit on <i>F</i> ²	1.152
Final <i>R</i> indexes [<i>I</i> > 2 σ (<i>I</i>)]	<i>R</i> ₁ = 0.0830, <i>wR</i> ₂ = 0.1802
Final <i>R</i> indexes [all data]	<i>R</i> ₁ = 0.1075, <i>wR</i> ₂ = 0.1963
Largest diff. peak/hole / e Å ⁻³	1.49/-0.81

Table S7. Selected bond lengths (Å) and angles (°) for **1**.

Fe1-S1	2.2820(12)	P1-C23	1.835(4)
Fe1-P1	2.2166(12)	P1-C17	1.833(4)
Fe1-N1	1.865(3)	S1-C11	1.751(4)
P1-C16	1.834(4)	N1-N1'	1.130(6)
P1-Fe1-S1	86.22(4)	C11-C16-P1	114.7(3)
N1-Fe1-S1	90.57(11)	C15-C16-P1	125.4(3)
N1-Fe1-P1	92.19(11)	C16-P1-Fe1	106.78(14)
N1-Fe1-C1	158.36(16)	C16-P1-C23	107.31(18)
N1-Fe1-C5	129.31(16)	C23-P1-Fe1	118.32(13)
N1-Fe1-C4	95.00(16)	C17-P1-Fe1	120.15(14)
N1-Fe1-C3	92.17(15)	C17-P1-C16	100.20(18)
N1-Fe1-C2	123.88(16)	C17-P1-C23	102.11(18)
C1-Fe1-S1	105.40(12)	N1'-N1-Fe1	177.3(4)
C1-Fe1-P1	103.17(12)	C3-Fe1-S1	148.13(12)
C5-Fe1-S1	88.05(12)	C3-Fe1-P1	125.36(12)
C5-Fe1-P1	138.16(13)	C2-Fe1-S1	144.97(13)
C4-Fe1-S1	107.95(12)	C20-Fe1-P1	97.47(12)
C4-Fe1-P1	163.99(12)	C11-S1-Fe1	105.48(14)

Table S8. Selected bond lengths (Å) and angles (°) for **5h**.

B1-N1	1.4208(19)	C6-C7	1.509(2)
B1-O1	1.3731(19)	C6-N1	1.4672(18)
B1-O2	1.3752(18)	C7-C8	1.389(2)
C1-C2	1.384(2)	C7-C12	1.400(2)
C1-C13	1.396(2)	C8-C9	1.389(2)
C2-C3	1.384(2)	C9-C10	1.380(3)
C3-C4	1.387(2)	C10-C11	1.384(2)
C4-C5	1.392(2)	C11-C12	1.404(2)
C5-C13	1.410(2)	C12-C13	1.473(2)
C5-N1	1.4197(17)		
O1-B1-N1	123.84(13)	C5-C13-C12	118.49(13)
O2-B1-N1	122.15(13)	C8-C7-C12	120.59(14)
C3-C2-C1	119.79(14)	C12-C7-C6	117.51(13)
C2-C3-C4	120.39(14)	C7-C8-C9	119.88(15)
C3-C4-C5	120.18(14)	C10-C9-C8	120.08(15)
C4-C5-C13	119.86(13)	C9-C10-C11	120.50(15)
C4-C5-N1	121.43(13)	C10-C11-C12	120.31(15)
C13-C5-N1	118.68(13)	C7-C12-C11	118.57(14)
N1-C6-C7	110.70(12)	C7-C12-C13	118.61(13)
C1-C13-C5	118.66(14)		

Table S9. Selected bond lengths (Å) and angles (°) for **6**.

C1-Fe1	2.097(5)	C32-C33	1.417(8)
C2-Fe1	2.109(4)	C33-C34	1.369(8)
C3-Fe1	2.121(5)	C34-C35	1.419(8)
C4-Fe1	2.120(5)	C35-C36	1.405(8)
C5-Fe1	2.098(5)	C36-C37	1.362(7)
C29-C30	1.432(7)	C37-N1	1.385(6)
C29-N1	1.318(7)	Fe1-N1	2.024(4)
C30-C31	1.397(8)	Fe1-P1	2.2105(15)
C30-C35	1.418(7)	Fe1-S1	2.2850(16)
C31-C32	1.378(8)		
C16-C11-S1	119.6(4)	N1-Fe1-P1	95.54(12)
C11-C16-P1	114.8(4)	N1-Fe1-S1	91.48(13)
N1-C29-C30	123.9(5)	P1-Fe1-S1	85.25(6)
C31-C30-C35	120.4(5)	C29-N1-C37	117.2(5)
C35-C30-C29	117.5(5)	C16-P1-C17	99.2(2)
C32-C31-C30	119.9(5)	C16-P1-C23	106.7(2)
C31-C32-C33	120.4(6)	C16-P1-Fe1	109.27(17)
C34-C33-C32	120.3(5)	C17-P1-C23	104.4(2)
C33-C34-C35	120.4(5)	C17-P1-Fe1	118.94(16)
C30-C35-C34	118.6(5)	C23-P1-Fe1	116.46(16)
C36-C35-C30	117.8(5)	C11-S1-Fe1	107.74(18)
C37-C36-C35	120.1(5)		

Table S10. Selected bond lengths (Å) and angles (°) for **7**

Fe1-N1	2.040(3)	Fe1-S1	2.2878(10)
Fe1-C1	2.096(3)	N1-C29	1.349(4)
Fe1-C5	2.104(3)	N1-C33	1.352(4)
Fe1-C2	2.114(3)	C29-C30	1.379(5)
Fe1-C4	2.116(3)	C30-C31	1.375(5)
Fe1-C3	2.122(3)	C31-C32	1.382(5)
Fe1-P1	2.2135(10)	C32-C33	1.377(5)
N1-Fe1-P1	92.58(7)	C16-C11-S1	120.7(2)
N1-Fe1-S1	92.42(8)	C11-C16-P1	115.1(2)
P1-Fe1-S1	86.08(3)	N1-C29-C30	123.6(4)
C11-S1-Fe1	106.48(11)	C31-C30-29	119.8(4)
C29-N1-C33	115.8(3)	C30-C31-C32	117.6(3)
C29-N1-Fe1	121.9(2)	C33-C32-C31	119.6(4)
C33-N1-Fe1	121.5(2)	N1-C33-C32	123.6(3)

Table S11. Selected bond lengths (Å) and angles (°) for **8**

Fe1-P1	2.2108(16)	Fe1-C25	2.099(6)
Fe1-S1	2.2896(18)	P1-C19	1.849(5)
Fe1-N1	2.004(5)	P1-C12	1.815(5)
P1-C13	1.833(6)	N1-C1	1.317(9)
S1-C7	1.750(6)	N1-C5	1.365(8)
P1-Fe1-S1	85.62(6)	N1-C5-C4	123.3(7)
N1-Fe1-P1	95.10(15)	C12-P1-C13	106.1(2)
N1-Fe1-S1	90.78(17)	C13-P1-Fe1	117.38(18)
N1-Fe1-C29	137.8(2)	C13-P1-C19	104.3(2)
N1-Fe1-C28	98.9(2)	C7-S1-Fe1	107.1(2)
N1-Fe1-C26	110.4(2)	C1-N1-Fe1	120.0(4)
N1-Fe1-C27	86.2(2)	C1-N1-C5	117.5(6)
N1-Fe1-C25	150.4(2)	C5-N1-Fe1	121.3(5)
C29-Fe1-P1	97.52(16)	N1-C1-C2	122.9(7)
C29-Fe1-S1	130.21(19)	C25-Fe1-C26	40.5(2)
C29-Fe1-C28	39.6(2)	C25-Fe1-C27	66.2(2)
C29-Fe1-C27	65.8(2)	C12-P1-C19	99.5(2)
C28-Fe1-P1	114.70(18)	C25-Fe1-C28	67.1(2)
C28-Fe1-S1	156.30(19)	C27-Fe1-P1	153.9(2)
C26-Fe1-P1	154.11(19)	C27-Fe1-S1	120.4(2)
C26-Fe1-S1	89.60(19)	C27-Fe1-C28	39.8(2)
C26-Fe1-C29	66.7(2)	C25-Fe1-P1	114.41(17)
C26-Fe1-C28	66.8(3)	C25-Fe1-S1	94.11(19)
C26-Fe1-C27	38.6(3)	C25-Fe1-C29	39.6(2)

12. Reference

- (1) Block, E.; Ofori-Okai, G.; Zubieta, J. *J. Am. Chem. Soc.* **1989**, *111*, 2327.
- (2) (a) Walter, M. D.; White, P. S. *New J. Chem.* **2011**, *35*, 1842; (b) Zhang, F.; Jia, J.; Dong, S.; Wang, W.; Tung, C.-H. *Organometallics* **2016**, *35*, 1151.
- (3) (a) Arrowsmith, M.; Hill, M. S.; Hadlington, T.; Kociok-Köhn, G.; Weetman, C. *Organometallics* **2011**, *30*, 5556; (b) Oshima, K.; Ohmura, T.; Suginome, M. *J. Am. Chem. Soc.* **2012**, *134*, 3699; (c) Intemann, J.; Lutz, M.; Harder, S. *Organometallics* **2014**, *33*, 5722.
- (4) Dudnik, A. S.; Victoria L. Weidner; Motta, A.; Delferro, M.; Marks, T. J. *Nat. Chem.* **2014**, *6*, 1100.
- (5) Palatinus, L.; Chapuis, G. *J. Appl. Crystallogr.* **2007**, *40*, 786.
- (6) Sheldrick, G. M. *Acta Crystallogr. Sect. C* **2015**, *71*, 3.
- (7) Dolomanov, O. V.; Bourhis, L. J.; Gildea, R. J.; Howard, J. A. K.; Puschmann, H. *J. Appl. Crystallogr.* **2009**, *42*, 339.
- (8) Spek, A. L. *Acta Crystallogr. Sect. D* **2009**, *65*, 148.
- (9) Complexes **9** and **10** have been reported in Song, H.; Ye, K.; Geng, P.; Han, X.; Liao, R.-Z.; Tung, C.-H.; Wang, W. *ACS Catal.* **2017**, *7*, 7709.
- (10) (a) MacNair, A. J.; Millet, C. R. P.; Nichol, G. S.; Ironmonger, A.; Thomas, S. P. *ACS Catal.* **2016**, *6*, 7217; (b) Labre, F.; Gimbert, Y.; Bannwarth, P.; Olivero, S.; Dunach, E.; Chavant, P. Y. *Org. Lett.* **2014**, *16*, 2366.